# USGS
science for a changing world

Prepared for the National Aeronautics and Space Administration

Geologic Map of the Beta Regio Quadrangle (V–17), Venus

By Alexander Basilevsky

Scientific Investigations Map 3023
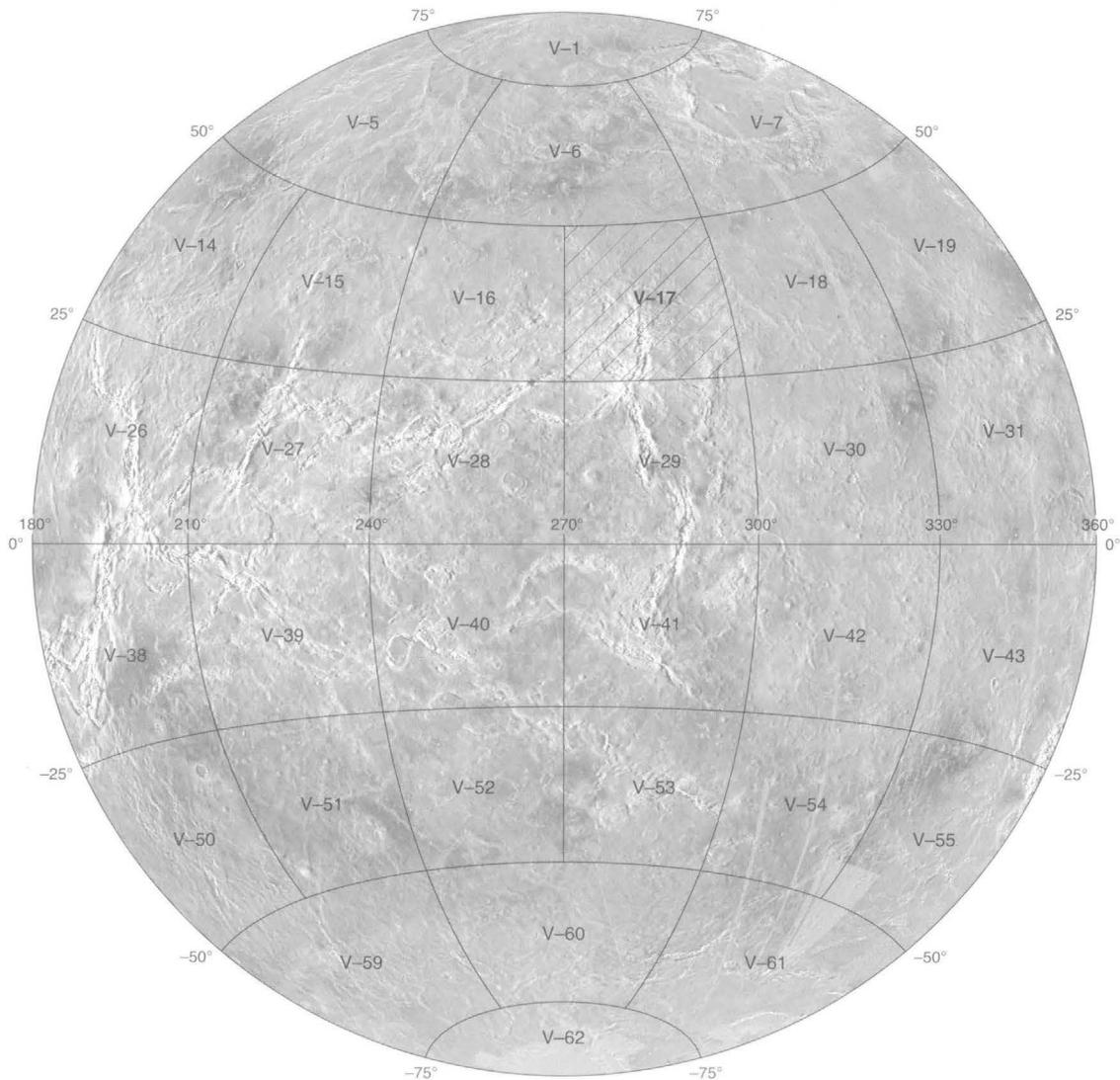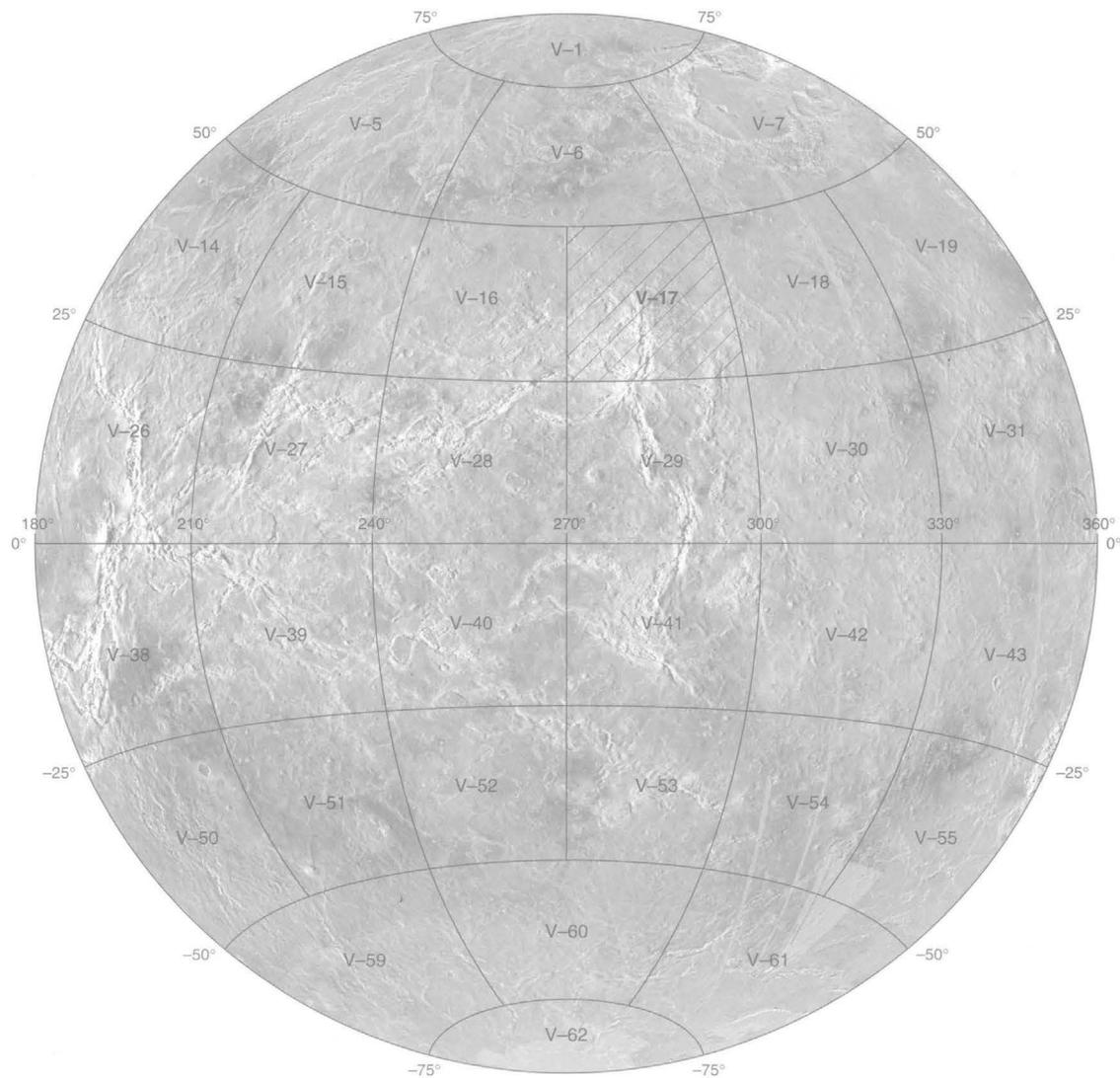
2008

U.S. Department of the Interior
U.S. Geological Survey

Geologic Map of the Beta Regio Quadrangle (V–17), Venus

By Alexander Basilevsky

2008

The Magellan Mission

The Magellan spacecraft orbited Venus from August 10, 1990, until it plunged into the Venusian atmosphere on October 12, 1994. Magellan Mission objectives included (1) improving the knowledge of the geological processes, surface properties, and geologic history of Venus by analysis of surface radar characteristics, topography, and morphology, and (2) improving the knowledge of the geophysics of Venus by analysis of Venusian gravity.

The Magellan spacecraft carried a 12.6-cm radar system to map the surface of Venus. The transmitter and receiver systems were used to collect three data sets: (1) synthetic aperture radar (SAR) images of the surface, (2) passive microwave thermal emission observations, and (3) measurements of the backscattered power at small angles of incidence, which were processed to yield altimetric data. Radar imaging, altimetric, and radiometric mapping of the Venusian surface was done in mission cycles 1, 2, and 3 from September 1990 until September 1992. Ninety-eight percent of the surface was mapped with radar resolution on the order of 120 meters. The SAR observations were projected to a 75-m nominal horizontal resolution, and these full-resolution data compose the image base used in geologic mapping. The primary polarization mode was horizontal-transmit, horizontal-receive (HH), but additional data for selected areas were collected for the vertical polarization sense. Incidence angles varied between about 20 and 45 degrees.

High resolution Doppler tracking of the spacecraft was done from September 1992 through October 1994 (mission cycles 4, 5, 6). Some 950 orbits of high-resolution gravity observations were obtained between September 1992 and May 1993 while Magellan was in an elliptical orbit with a periapsis near 175 kilometers and an apoapsis near 8,000 kilometers. An additional 1,500 orbits were obtained following orbit-circularization in mid-1993. These data exist as a 75 degree by 75 degree harmonic field.

Magellan Radar Data

Radar backscatter power is determined by the morphology of the surface at a broad range of scales; and the intrinsic reflectivity, or dielectric constant, of the material. Topography at scales of several meters and larger can produce quasi-specular echoes, with the strength of the return greatest when the local surface is perpendicular to the incident beam. This type of scattering is most important at very small angles of incidence, since natural surfaces generally have few large tilted facets at high angles. The exception is in areas of steep slopes, such as ridges or rift zones, where favorably tilted terrain can produce very bright signatures in the radar image. For most other areas, diffuse echoes from roughness at scales comparable to the radar wavelength are responsible for variations in the SAR return. In either case, the echo strength is also modulated by the reflectivity of the surface material. The density of the upper few wavelengths of the surface can have a significant effect. Low-density layers such as crater ejecta or volcanic ash can absorb the incident energy and produce a lower observed echo.

On Venus, there also exists a rapid increase in reflectivity at a certain critical elevation, above which high-dielectric minerals or coatings are thought to be present. This leads to very bright SAR echoes from virtually all areas above that critical elevation.

The measurements of passive thermal emission from Venus, though of much lower spatial resolution than the SAR data, are more sensitive to changes in the dielectric constant of the surface than to roughness. As such, they can be used to augment studies of the surface and to discriminate between roughness and reflectivity effects. Observations of the near-nadir backscatter power, collected using a separate smaller antenna on the spacecraft, were modeled using the Hagfors expression for echoes from gently undulating surfaces to yield estimates of planetary radius, Fresnel reflectivity, and root-mean-square (rms) slope. The topographic data produced by this technique have horizontal footprint sizes of about 10 km near periapsis, and a vertical resolution on the order of 100 m. The Fresnel reflectivity data provide a comparison to the emissivity maps, and the rms slope parameter is an indicator of the surface tilts, which contribute to the quasi-specular scattering component.

Introduction

Physiography

The Beta Regio quadrangle (V–17) is in the northern hemisphere of Venus and extends from latitude 25° to 50° N. and from longitude 270° to 300° E. (figs. 1, 2). Its southern part covers a significant part of the prominent and generally domal topographic rise of Beta Regio and the northern area of the less prominent and generally flat topped rise of Hyndla Regio. Part of the lowland plains of Guinevere Planitia, most of which is below the 6,051 km datum, occupies the northern part of the quadrangle. Within the plains but close to the northeastern part of the Beta Regio rise there is a radiating system of radar-bright lineaments and grooves centered at Wohpe Tholus. The Beta Regio rise has two summits: Rhea Mons and Theia Mons, both of which reach altitudes more than 5 km above the datum. Rhea Mons is completely within the V–17 quadrangle. Only the northern part of Theia Mons is in the quadrangle. From north to south the Beta Regio rise is cut by the very prominent topographic trough of Devana Chasma, the deepest parts of which locally reach the altitude levels of the Guinevere Planitia. At the eastern and western flanks of Beta Regio rise, correspondingly, are the troughs of Aikhylu Chasma and Latona Chasma, which topographically are much less prominent than Devana Chasma. Close to Aikhylu Chasma there is a channel-like feature named Omutnitsa Vallis. The northern part of the Beta Regio rise is marked by the fracture belt of Agrona Linea.

Both within the upland and lowland parts of the quadrangle there are several isolated massifs of tesserae: Senectus, Lachesis, and Zirka in the eastern part of the quadrangle; Sudenitsa, in the west; and several unnamed massifs in the central part (fig. 1). As will be shown, only part of them are blocks of tes-

sera terrain, whereas others are composed of other geologic units although they somewhat resemble typical tessera terrain. Within the V–17 quadrangle there are also three topographically positive deformation belts: Dodona Dorsa, Iyele Dorsa, and Shishimora Dorsa. Four coronae are also present in the quadrangle; these are Rauni Corona, Urash Corona, Emegen Corona, and Blathnat Corona. In summary, the V–17 quadrangle is an interesting area for the analysis of the major geologic processes responsible for the observed morphology on the surface of Venus.

Previous Work

Beta Regio is one of a few regions of Venus that have been observed by Earth-based radar observations since 1964 (for example, Goldstein, 1965, 1967; Goldstein and Rumsey, 1972; Goldstein and others, 1978). Even at that time it was correctly concluded that its surface is rough but its geologic nature was unknown.

In 1975 the Venera 9 probe landed on the northeastern flank of Beta Regio rise (Keldysh, 1979; Moroz and Basilevsky, 2003). The gamma spectrometer measurements showed that in its contents of K, U, and Th, the surface material at the landing site (31.01° N., 291.64° E.) is close to terrestrial basalts (Surkov and others, 1976; Surkov, 1997). The spacecraft landed on a steep (approximately 30°) slope covered with talus of decimeter-sized fragments of rocks (Florensky and others, 1977; Keldysh, 1979).

The Pioneer-Venus radar studies, started in 1978, showed Beta Regio quadrangle in global context. Together with later and more sophisticated Earth-based radar observations they showed that Beta Regio is an area of inter-related rifting and volcanism (Masursky and others, 1980; McGill and others, 1981; Schaber, 1982; Campbell and others, 1984; Stofan and others, 1989). Devana Chasma was interpreted to be a part of global-wide system of rifts resembling terrestrial continental rifts (McGill and others, 1981; Schaber, 1982). Theia Mons, dominating the central part of Beta Regio rise, based on its topographic shape and radially extending flow-like radar-bright features, was interpreted as a large shield volcano (Masursky and others, 1980; Campbell and others, 1984; Stofan and others, 1989). Rhea Mons, dominating the northern part of Beta Regio, based on its topography, the presence of flanking radar-bright deposits, and radar-dark oval feature at its summit, interpreted to be a caldera, was considered a volcano split by Devana Chasma rift (Masursky and others, 1980; Campbell and others, 1984; Stofan and others, 1989).

The northern part of Beta Regio quadrangle was covered by the Venera 15/16 radar survey (Barsukov and others, 1984; Alexandrov and others, 1986; Kotelnikov and others, 1989) including SAR imaging with 1- to 2-km resolution. Photogeologic analysis of the images of the northern slope of Rhea Mons as well as the northern, northeastern, and northwestern flanks of the Beta Regio rise showed that the upper part of Rhea Mons is composed of the rough-surfaced unit resembling in its morphology tessera terrain, whereas within the lower standing Beta Regio flanks the smooth-surfaced unit dominates (Basilevsky,

1988; Sukhanov and others, 1989). Thus it was concluded that the northern part of the Beta Regio rise was mainly the result of the tectonic doming, whereas volcanism played a secondary role smoothing the uplift flanks. The joint analysis of the Pioneer Venus radar reflectivity and roughness data and the Venera 15/16 images permitted the prediction of the global distribution of tessera terrain (Kreslavskii and others, 1989; Bindschadler and others, 1990). According to this prediction, Rhea Mons and several other areas within the Beta Regio rise with high probability were considered tessera terrain.

Magellan observations provided the most complete high-resolution data for Beta Regio, including 120–220 m/pixel SAR images (Saunders and others, 1992; Solomon and others, 1992; Senske and others, 1992). The global Venus tectonic overview by Solomon and others (1992) as well as a more regional study by Senske and others (1992) confirmed the early interpretation of Theia Mons as a large shield volcano superposed on the Devana Chasma rift and added the observation that this volcano was partly cut by later rifting faults. These researchers also found the rift in northern Beta Regio surrounded by tessera, and their discovery confirmed the prediction by Kreslavskii and others (1988) and Bindschadler and others (1990). Rhea Mons, the northern summit of Beta Regio, was interpreted as an area of tessera terrain with some smooth plains of possible volcanic origin (Solomon and others, 1992; Senske and others, 1992). The analysis also revealed the 37-km crater Balch cut by the north-trending rift faults and extended by rifting in an easterly direction by about 10 km. To the north of Beta Regio rise at the boundary with Guinevere Planitia, a zone of faults and grabens trending generally east was observed (Agrona Linea) and interpreted as cutting faults extending from Devana Chasma (Solomon and others, 1992).

The south half of the V–17 quadrangle has been covered by the study of Ivanov and Head (2001a) who, based on the analysis of the Magellan data, geologically mapped a global geotraverse at 30° N. latitude. This study, which covered 20 contiguous Magellan C1-MIDRs, had mostly stratigraphic and partly structural emphasis and thus is closely related to the V–17 mapping project. The authors of that study tested and modified the regional and global stratigraphy of Venus worked out by Basilevsky and Head (1995a,b, 1998, 2000) and Basilevsky and others (1997) as a starting point and added new units. Within the southern part of the V–17 quadrangle, Ivanov and Head (2001a) identified and mapped eleven geologic units: nine stratigraphic material units and two structural units. The mapped stratigraphic units (from older to younger) are: (1) tessera terrain material (t), (2) material of densely fractured plains (pdf), (3) material of fractured and ridged plains (pfr), (4) material of shield plains (psh), (5) material of plains with wrinkle ridges (lower unit pwr_1), (6) material of plains with wrinkle ridges (upper unit pwr_2), (7 and 8) materials of lobate (pl) and smooth (ps) plains, and (9) undivided impact crater materials (cu), whose age could be correlative with any of the above eight units. The two structural units are represented by older fracture belts (fb) and younger rifted terrain (rt), considered correspondingly as areas of the older and younger rifting.

For the part of the V–17 quadrangle covered, their mapping showed the presence of several medium-sized (hundreds of kilo-

meters across) massifs of tessera. In between they mapped areas of the pdf, pfr, psh, and pwr units with an unusual dominance of psh over pwr. In agreement with the results of Solomon and others (1992) and Senske and others (1992), Rhea Mons was interpreted by Ivanov and Head (2001a) as an uplifted block of tessera cut by the Devana Chasma rift (rt) whereas Theia Mons was interpreted as a volcano made of the lobate plains material (pl). Their mapping also showed presence of the fracture belts (fb) along the northern part of Beta Regio rise (Agrona Linea). Contrary to the interpretation of Solomon and others (1992), these fracture belts were determined to be older than Devana Chasma structures. Ivanov and Head (2001a) noted that most the elevated areas within the Beta Regio were made up of a collection of older units predating plains with wrinkle ridges (pwr). From this finding, they concluded that Beta Regio was high standing before the emplacement of pwr plains.

In their study Ivanov and Head (2001a) identified a new type of terrain characterized by "a pattern of tectonic deformation that fits the formal definition of tessera (two sets of almost orthogonally cross-cutting structures). However this terrain is less deformed than typical tessera and some of the material of the unit appears to embay tessera massifs" (Ivanov and Head, 2001a, p. 17,549). They found that this terrain was formed as a result of additional deformation of densely fractured plains (pdf) and fractured and ridges plains (pfr) and named it "tessera transitional terrain" (tt). They did not show tt as a separate unit on the map but briefly described its distribution within the geotraverse, including the covered part of the V–17 quadrangle, where it formed at the expense of pfr.

Basilevsky and Head (2002a) used the degree of degradation of crater-associated radar-dark haloes on Venus to estimate the age of the crater and neighboring units in fractions of T, the mean global surface age of Venus. The halo-degradation technique was applied to several regions of the planet including Beta Regio. For five craters within the Beta rise (Sanger, Olga, Raisa, Tako, and Balch) the degree of degradation of crater-associated dark haloes and the relations of these craters to the neighboring volcanic and tectonic units and features has been determined. It was found, in particular, that ejecta outflows of the crater Sanger, which sits on the eastern slope of the Beta Regio rise and has a clear dark halo (crater age is <0.5T), are cut by the faults branching from the Devana Chasma rift. This relation implies that the Devana rift was active at least 0.5T ago and may be even subsequent to that time (Basilevsky and Head, 2002a).

Ernst and others (2003) mapped graben-fissure systems in a broad region, the central part of which is the V–17 area. In this region they identified 79 such systems and classified them into radiating (34), linear (26), and circumferential (19). A significant part of these systems lies within the V–17 quadrangle: 9 radiating, 11 linear, and 5 circumferential. They found that many of the systems are (1) younger that t, pdf, and pfr units, (2) coeval with, and in many cases define, fracture belts, (3) partially flooded by pwr plains, and (4) older than pl–ps plains and young (rt) rifts. Ernst and others (2003) also found that many of the radiating systems have a central topographic uplift and extend well beyond it, and this relation implies that grabens and fissures are underlain by dikes.

Beta Regio belongs to the category of large Venusian topographic rises, which are called "volcanic rises" because they encompass large volcanoes. Pioneer Venus and then Magellan observations showed that Beta Regio is characterized by an extremely high amplitude anomaly in geoid and gravity (+110 m, +150 mgal), a large ratio of geoid to topography, and apparent depth of compensation in the range of 225 to 400 km. These characteristics imply that the Beta Regio rise (like other volcanic rises) is a hotspot or the surface manifestation of mantle upwelling (see for example, Phillips and Malin, 1983; Phillips and others, 1991; Bindschadler and others, 1992a; Herrick and Phillips, 1992; Konopliv and Sjogren, 1994; Solomatov and Moresi, 1996; Smrekar and others, 1997; Hansen and others, 1997; Konopliv and others, 1999).

Smrekar and others (1997) divided the Venusian hot spots into three types: (1) rift-dominated, (2) volcano-dominated, and (3) corona-dominated, and they classified Beta Regio as a rift-dominated hot spot. Foster and Nimmo (1996) compared the rift system of Beta Regio to parts of the East African rift. According to these authors both rift systems have effective elastic thickness of approximately 30 km and maximum fault segment lengths of approximately 100 km. These rift systems differ, however, in the maximum width of their half graben: approximately 150 km for Beta Regio and approximately 50 km for East Africa. The larger width of the Venusian rift suggests that the faults bounding it are stronger than faults of the East African rift. This strength may be due to the enhanced dryness of Venusian rocks that makes them mechanically very strong (Mackwell and others, 1995, 1998).

Leftwich and others (1999) made a spectral correlation analysis of observed free-air anomalies calculated for three large regions of Venus, including Beta Regio. The model for Beta Regio suggests a thickened (≥40 km) crust relative to the surrounding plains, and it suggests a thinner crust beneath the Devana Chasma rift zone. According to this analysis, Beta Regio may be thermodynamically supported by mantle upwelling or have a thickened crust that is not yet completely compensated. The authors conclude that Beta Regio rise may be volcanically active at present or perhaps volcanism ceased in geologically recent times.

Rathbun and others (1999) used Magellan altimetry, gravity, and SAR images to constrain some parameters important in the formation of the Beta Regio rise. Using altimetry data and a fault-dip angle derived from the split of crater Balch, they determined the extension in the rifts of this region and then estimated the hoop strain (from 0.1 to 2 percent) accommodated by the rifts from the extension in these rifts. Using two separate modeling techniques, they then compared the observed and modeled gravity and uplift for this area and concluded that a relatively low density contrast region now exists below Beta Regio and has caused the uplift and rifting.

The formation of Beta Regio rise due to uplift caused by a mantle plume was modeled by Vezolainen and others (2003, 2004). In the first of these two works, a two-dimensional modeling was undertaken. The model predicts correct gravity and topography anomalies and fast uplift time for Beta Regio (approximately 500 m.y.), which agrees with the geologic constraints (Basilevsky and Head, 2002a; Basilevsky and others,

2003). However, in this model the fast uplift requires very low viscosity of the lithosphere beneath Beta Regio rise that is difficult to reconcile with the experimental data on the rheology of dry rocks (Mackwell and others, 1995, 1998). If the upper crust is made realistically strong, the uplift time becomes about 1.2 b.y., which is only marginally acceptable from both geologic and geodynamic points of view (Vezolainen and others, 2003). Either for some reason the lithosphere is indeed very weak there or the model needs to be modified.

Vezolainen and others (2004) explored using three-dimensional (3-D) modeling. This model satisfies constraints on gravity, topography, rheology, and the uplift rate substantially better than the two-dimensional model. The uplift time is reduced to an acceptable 800 m.y. The 3-D model gives the plume formation depth to be around 3,000 km, that is, approximately the mantle-core boundary. The model results depend only weakly on the initial lithosphere thickness so the thick present-day lithosphere (approximately 400 km) can be reconciled with a thin lithosphere at the time of global resurfacing (100–200 km) inferred from the melt generation rates and the flexural rigidity models (Vezolainen and others, 2004). Both models imply that the Beta Regio rise may still be growing.

Mapping Approach

The geologic mapping of the V–17 Beta Regio quadrangle used traditional methods of geologic unit definition and characterization for the Earth (for example, American Commission on Stratigraphic Nomenclature, 1961) and planets (for example, Wilhelms, 1990) appropriately modified for radar data (Tanaka, 1994). Unit definitions and mapped key relations are based on the full resolution Magellan synthetic aperture radar (SAR) data (mosaicked full-resolution basic image data records, C1-MIDR's, F-MIDR's, and F-Maps). These results have been transferred to the base map compiled at a scale of 1:5 million. In addition to the SAR image data, digital versions of Magellan altimetry (including U.S. Geological Survey pseudo-stereo images), emissivity, Fresnel reflectivity, and roughness data (root mean square, rms, and slope) were used. During this project, a convenient source of the data the U.S. Geological Survey provides was also used (namely, http://pdsmaps.wr.usgs.gov/PDS/public/explorer/html/fmappick.htm). The background for unit definition and characterization is described in Tanaka (1994), Basilevsky and Head (1995a, b; 2000), Basilevsky and others (1997), Hansen (2000), and Ivanov and Head (2001a).

Magellan Sar and Related Data

In this mapping project the images taken by the synthetic aperture radar (SAR) instrument (12.6 cm, S-band) flown on the Magellan spacecraft were used. They represent a record of the radar echo returned to the spacecraft antenna, which is influenced by surface composition, slope, and wavelength-scale surface roughness. Viewing and illumination geometry also influence the appearance of surface features in SAR images. For the V–17 quadrangle, only left-look Magellan images were acquired. Guidelines for geologic mapping using Magellan SAR images and their interpretation can be found in Elachi (1987), Saunders and others (1992), Ford and Pettengill (1992), Tyler and others (1992), and Tanaka (1994). In the area of the Beta Regio quadrangle, incidence angles are such that backscatter is dominated by variations in surface roughness at wavelength scales. Rough surfaces appear relatively bright, whereas smooth surfaces appear relatively dark. At the same time within the areas of approximately the same and not high surface roughness the surface slopes are easily seen. Variations also occur depending on the orientation of features relative to the incident radiation (illumination direction), with features normal to the illumination direction being more prominent than those oriented parallel to it. Full-resolution images have a pixel size of 75 m; C1-MIDR's contain the SAR data displayed at approximately 225 m/pixel. Altimetry data were of great importance in establishing geologic and stratigraphic relations between units too. Also essential in the analysis of the geology of the surface are data obtained by Magellan on the emissivity (passive thermal radiation), reflectivity (surface electrical properties), and rms slope (distribution of radar wavelength scale slopes). Aspects of these measurements were used in unit characterization and interpretation; background on the characteristics of these data and their interpretation can be found in Saunders and others (1992), Ford and Pettengill (1992), Tyler and others (1992), Tanaka (1994), and Campbell (1995).

General Geology

Two major geologic processes, volcanism and tectonism, have influenced the Beta Regio quadrangle to form most of the observed geologic features. Volcanism was found to be the dominant process of crustal formation on Venus (Head and others, 1992) and also in the formation of the observed geologic units in this map area. Tectonic activity has modified some of these materials (for example, Solomon and others, 1992; Squyres and others, 1992) in a variety of modes of strain (extensional, contraction, and shear), and in places deformation is so extensive, as in the case of tessera terrain, that the deformational features become part of the definition of the material unit (see also Tanaka, 1994; Campbell and Campbell, 2002, Hansen and DeShon, 2002; Stofan and Guest, 2003; Ivanov and Head, 2004; Brian and others, 2005). Impact cratering also has locally influenced some areas in the quadrangle but has not been an influential process over the quadrangle as a whole (fig. 1). Aeolian processes did operate within the V–17 quadrangle but their signatures here are insignificant (Greeley and others, 1997). Steep slopes, especially in Devana Chasma rift and associated grabens and faults, created conditions for dowslope mass movement, including rock/debris avalanches (Malin, 1992). Atmosphere-surface interactions are apparently visible within the V–17 quadrangle in the form of areas of high reflectivity and low emissivity above approximately +4 km altitude (Klose and others, 1992).

Volcanic processes within the quadrangle formed four major types of the deposits. The first type is represented by

the materials forming regional plains with relatively smooth primary surfaces (Head and others, 1992; Guest and others, 1992; Basilevsky and others, 1997). They dominate within the Guinevere Planitia in the northern part of the quadrangle and in isolated areas in the southern part of it where they form the four members of the plains with wrinkle ridges (pwr1, pwr2, pwr3, pwru). The second type of deposit is material that forms fields of numerous small gentle-sloping shields (Aubele and Slyuta, 1990; Head and others, 1992; Guest and others, 1992; Aubele, 1994, 1995; Crumpler and others, 1997). These shields dominate in the eastern and southern parts of the V–17 quadrangle, especially within relatively low altitude parts of the Beta Regio rise, where they form the unit of shield plains (psh). The third type is represented by flows seen on the slopes of Theia Mons volcano (Head and others, 1992; Crumpler and others, 1997) that form the unit of lobate plains (pl). These flows are also observed in several other places of the quadrangle but with no association with prominent volcanic edifices. The fourth type consists of small fields of radar-dark, morphologically smooth material that locally form very gentle sloping shields with summit pits. These fields typically have narrow extensions that make them appear similar to amoeba and, in fact, were called "amoeboids" by Head and other (1992). These lavas form in the regional-scale unit of smooth plains (ps). In addition, materials that probably formed due to volcanic activity, but whose volcanic origin is partly or significantly masked by tectonic deformation, are present in many isolated areas of the quadrangle and form units of fractured and ridged plains (pfr), densely fractured plains (pdf) and possibly tessera (t) (Basilevsky and Head, 1995a,b, 2000; Ivanov and Head, 2001a).

Tectonic processes within the V–17 quadrangle are manifested in several ways. The most prominent result is the Beta Regio rise, whose origin owing to tectonic domal uplift is now accepted (for example, Solomon and others, 1992; Senske and others, 1992; Hansen and others, 1997; Rathbun and others, 1999; Vezolainen and others, 2004). The Devana Chasma, considered a rift zone (for example Masursky and others, 1980; McGill and others, 1981; Stofan and others, 1989; Solomon and others, 1992; Senske and others, 1992; Hansen and others, 1997), is undoubtedly another product of tectonic activity in the quadrangle. The most heavily deformed parts of Devana Chasma and a few associated zones of smaller size have been mapped as tectonic unit r. The long east-trending belt of faults and fractures, including Agrona Linea and Shishimora Dorsa, is another product of tectonism in the area. These faults and fractures have been mapped as tectonic unit fb. In close association with Agrona Linea there are four coronae (Rauni, Urash, Emegen, and Blathnat) and four radiating systems of faults (so called "astra"). All of these features are of likely tectonic origin. Most of them (except the radiating system centered at Wohpe Tholus) have been shown on the geologic map as areas of unit fb. Tectonic deformation is responsible for the structure and morphology of one more tectonic unit: tessera transitional terrain (tt) that formed as a result of moderately dense faulting of units pfr and pdf.

Tectonic deformation significantly influenced the structure and morphology of two geologic units: tessera terrain (t) and densely fractured plains (pdf). Less intense tectonic deforma-

tion influenced fractured and ridged plains (unit pfr), shield plains (unit psh) and plains with wrinkle ridges (pwr). The youngest geologic units, namely lobate plains (pl) and smooth plains (ps), are only locally influenced by tectonic deformation.

Impact cratering within V–17 quadrangle resulted in the formation of 25 craters with diameters from 1.3 to 84 km (Schaber and others, 1998) and 3 splotches (fig. 1, table 1). Most of the craters are superposed on different geologic units of the area, and only a few of them are superposed by relatively young tectonic structures and volcanic lavas. The largest craters of the quadrangle show not only hummocky ejecta typical of Venusian impact craters but also ejecta outflows. Deposits of the fine fraction of the crater ejecta are seen around 21 of 25 craters of this area in the form of radar-dark haloes (fig. 3). The degree of preservation of crater-associated radar-dark haloes (Arvidson and others, 1992; Herrick and Phillips, 1994; Basilevsky and Head, 2002a; Basilevsky and others, 2003) and crater relations with neighboring geologic units and features were used to divide the craters of the V–17 quadrangle into three age categories.

Signatures of eolian processes are rather rare within the V–17 quadrangle. These processes require a debris source to produce deposits or friable material to be a subject of deflation (Greeley and others, 1997) so they often are in association with impact craters. Within the V–17 quadrangle the work of eolian processes can be inferred from the different degrees of preservation of the radar-dark crater-associated deposits (fig. 3) (see for example, Basilevsky and Head, 2002a; Basilevsky and others, 2003) and can be seen in the form of local patches of radar-dark deposits not associated with craters but localized in windshadow locations (fig. 4).

In theV–17 quadrangle, features that formed owing to downslope mass wasting on rather steep slopes can be seen both on SAR images (in the form of groove-like features and talus fans in Devana Chasma rift) and on the Venera 9 TV panorama in the form of rock-fragment talus (both examples are shown in fig. 5).

Atmosphere-surface interaction within the V–17 quadrangle led to a significant increase in its reflectivity and decrease in emissivity above approximately +4 km altitude level probably owing to changes of mineral composition of the surface material (Klose and others, 1992).

Stratigraphy

Venus is a planet with a relatively small (approximately 1,000) number of impact craters on its surface. This paucity of craters makes it possible to estimate a mean surface age of the planet and mean ages of a few globally distributed geologic units, but not the ages of units and features of rather small areas, which contain a small number of craters. The estimate of the mean surface age of the planet is approximately 750 m.y., but values between 300 m.y. and 1 b.y. are considered possible (McKinnon and others, 1997). This estimate is practically equal to the estimate of the global mean for the regional plains, which correspond to combination of units psh and pwr described herein (Basilevsky and Head, 2000). Within the V–17 quad-

rangle there are 25 impact craters (Schaber and others, 1998). With the total area of the quadrangle being approximately 6 x 10^6 km^2, their mean areal density is approximately 4 craters per 10^6 km^2, which is about two times greater than the global mean (approximately 2 craters per 10^6 km^2). However this can not be a reliable indication of a relatively old mean surface age of the study region because a simple statistical test shows that for 95 percent (2σ) confidence level, the density estimate for the V–17 quadrangle lies within 2.5 to 6 craters per 10^6 km^2 and for 99.7 percent (3σ) confidence level it is 1.7 to 6.7 per 10^6 km^2. So the difference between the mean age for the V–17 quadrangle and mean surface age for the planet is not reliable.

Crater areal densities on different geologic units within the V–17 quadrangle cannot be used for estimating their relative ages. Therefore, to establish the geologic history of the region, the analysis of crosscutting, embayment, and superposition relations among the units and structures as well as the degree of preservation of crater-associated radar-dark haloes were used. The crater-associated halo approach provided the possibility of assessing if a given crater formed within the first or the second halves of post-regional-plains time (Basilevsky and Head, 2002a; Basilevsky and others, 2003), and then, from the analysis of age relation between this crater and the surrounding units and structures, to assess the age of the surrounding units and structures.

In the study area eight geologic material units, two of which are divided into members, have been mapped. Seven units form the time sequence. One unit (impact crater materials) is usually mapped as extending throughout the entire time period (Campbell and Campbell, 2002; Hansen and De Shon, 2002; Ivanov and Head, 2004), but this study resulted in the subdivision of the unit into three members of different ages. The requirement for units is distinct characteristics and age relations with other units adjacent to them both in space and time and this was the major criterion for unit identification. Typically the identified units and members maintain some specific morphology along the areas of their appearance, but morphologic similarity alone was not considered sufficient for unit identification. Age relations with other units and structures have always been used as a criterion. In the case of the crater materials unit, the degree of crater-associated dark-halo development and preservation was used to subdivide it into two subunits; one more subunit of crater materials has been identified on the basis of age relations with other neighboring geologic units.

Tectonic structure has been mapped independent of geologic units, but in some cases tectonic features are such a pervasive part of the morphology of the terrain that they become part of the definition of a unit at this scale. For example, the tessera unit (t) and densely fractured plains unit (pdf) are so saturated with faults that at the Magellan SAR resolution the undeformed materials of these units are practically invisible. However, the U.S. Geological Survey has accepted the mapping of these units as material units on Venus. See maps by Bender and others (2000) and Brian and others (2005) for examples.

In some cases structures have been used as one of the steps in the unit identification even if the density of structures was not very great. For example, the unit of plains with wrinkle ridges (pwr) is characterized by these ridges in practically all of its mapped localities. The undeformed material of the unit is easily seen and it is evident that wrinkle ridges are superposed on it. The association of these ridges with this material unit is so typical that their presence was used as a part of the unit definition. A situation similar to this is the unit of fractured and ridged plains (pfr); in most localities of this unit, broad ridges are observed and are morphologically very different from wrinkle ridges.

However, we emphasize that structures were used for unit identification only as only one of the steps. Other morphological characteristics and age relations with other units were the predominant step in determining unit identification. For example, in some places of the Devana Chasma rift zone, faults are very dense and criss-crossed so the resulting morphology is somewhat similar to that of tessera terrain. But these faults obviously cut the adjacent regional plains while tessera is embayed by them. So this rift terrain subarea is not confused with the older tessera unit and is thus not mapped as unit t. Sometimes the surface of fractured and ridged plains (pfr) is locally deformed by wrinkle ridges so as to look in this subarea to be part of unit pwr. However, examination of the stratigraphy shows that this wrinkle-ridged material is deformed also by the wide ridges typical for unit pfr and is embayed by the lower member of pwr plains. These two observations allow this pfr plains subarea to be distinguished from pwr plains.

In some areas of the V–17 quadrangle there are structural zones in which it is possible to understand age relations with neighboring units, but because of the high density of the structures it is difficult, if not impossible, to judge what material is deformed within the zones. In these cases tectonic units were identified. Age of tectonic units is related to age of the deformation, not to age of deformed material. Their boundaries are typically gradual and thus outlined rather arbitrarily. Three tectonic units have been identified within the V–17 quadrangle and are described in the "Description of Map Units."

This approach of unit identification strictly follows the guidelines on planetary geologic mapping (Wilhelms, 1990) and in particular on the geologic mapping of Venus (Tanaka, 1994) and is generally similar to the approach used by other mappers, although in relation of concrete units and structures, differences of opinion exist (see Bender and others 2000; DeShon and others, 2000; Ivanov and Head, 2001a,b; Rosenberg and McGill, 2001; Bridges and McGill, 2002; Campbell and Campbell, 2002; Hansen and DeShon, 2002; Brian and others, 2005). The stratigraphic units and structures and their relations are summarized in the "Description of Map Units."

Tessera material (unit t, fig. 6). This unit is interpreted to be the stratigraphically oldest unit in the quadrangle. It is embayed by most of the other units within the map area. Tessera terrain is radar bright, consists of at least two sets of intersecting ridges and grooves, and is a result of tectonic deformation of some precursor terrain (Barsukov and others, 1986; Basilevsky and others, 1986; Bindschadler and Head, 1991; Sukhanov, 1992; Solomon and others, 1992; Hansen and others, 1997). According to Ivanov (2001), in some rare localities (outside the V–17 quadrangle) it is possible to see that a precursor of tessera terrain is plains. Within V–17, as with other regions of Venus, ridges and grooves on the tessera surface show a

spectrum of spacing from a few hundred meters to several kilometers with wider features consisting of clusters of smaller ones. Undeformed parts of tessera material are not present in the V–17 quadrangle. Tessera unit occupies approximately 5 percent of the quadrangle (table 2), which is slightly smaller than the global abundance (8 percent) of this unit (Ivanov and Head, 1996). Within V–17, tessera unit forms two rather large blocks about 1,000 to 1,500 km long and 400 to 500 km wide. One block is about 1,500 km northwest of Rhea Mons, and the other is on the western flank of this mountain massif. Several blocks of a few hundred kilometers across and about 20 blocks of a few tens of kilometers across are also present in the V–17 quadrangle. Within the study area there are four physiographic units called tessera (Lachesis, Zirka) or tesserae (Senectus, Sudenitsa), but only the northern part of Sudenitsa Tesserae is partly composed of tessera unit whereas others are composed of other units.

Densely fractured plains material (unit pdf, fig. 7). Next in the time sequence is densely fractured plains material, which is characterized by relatively flat surfaces on a regional scale and by swarms of parallel and subparallel lineaments (sometimes resolved as fractures). Typical spacing of these lineaments is less than 1 km. However, because the pdf terrain is often intimately intermixed with undeformed volcanic material (usually it is unit psh) the greater lineament spacing was observed in some places. Although the unmodified precursor terrain for the densely fractured plains material is not observed, the flatness suggests that it was plains and based on analogy with the younger and less deformed plains of Venus, it could be volcanic plains made of mafic lavas (Basilevsky and Head, 2000). The pdf fractures are structural elements, but they are such a pervasive part of the morphology of this terrain that they become a key aspect of unit definition. Densely fractured plains are embayed by almost all younger material units, except the youngest units pl and ps, with which they are not observed in direct contact. In rare occurrences where pdf plains and tessera are in direct contact, the first one embays the second (fig. 8). Densely fractured plains occupy approximately 5 percent of the quadrangle (table 2), close or slightly greater than its 3 to 5 percent global abundance estimated by Basilevsky and Head (2000). It predominantly occurs in the northeastern part of quadrangle composing Senectus and Lachesis Tesserae. Small patches of pdf plains also occur in other parts of V–17 quadrangle.

Fractured and ridged plains material (unit pfr, fig. 9). This unit, next in the time sequence, is composed of medium-bright material with a predominantly smooth surface. In this aspect, unit pfr is similar to the younger units pwr (member 2) and pl, which bear morphologic evidence that they are composed of mafic lavas. So one may suggest that unit pfr is also composed of mafic lavas. But contrary to units pwr and pl, the pfr unit is commonly deformed by broad (3- to 10-km wide) ridges tens of kilometers long that form so-called ridge belts. Unit pfr embays the older units t and pdf and is embayed by the younger units psh, pwr, and pl (figs. 9, 10). Unit pfr in slightly or moderate deformed state composes approximately 5 percent of the V–17 quadrangle (table 2), similar to the 3 to 5 percent global abundance estimated by Basilevsky and Head (2000). It predomi-

nantly occurs in the south half of the V–17 quadrangle in the form of rather small, elongated zones separated from each other by the younger plains. In the north half of V–17 quadrangle, the pfr unit is also present but is significantly less abundant. Because it is deformed by faults and grabens, unit pfr makes up the predominant part of the tectonic unit tt.

Shield plains material (unit psh, figs. 6–11). Next after the fractured and ridged plains is the material of shield plains. It is typically of intermediate radar brightness and characterized by abundant, gently sloping shield-shaped features of a few kilometers in diameter, often with summit pits. Clusters of small shields were first recognized on the Venera 15/16 images (Barsukov and others, 1986; Aubele and Slyuta, 1990) and then with greater detail on Magellan SAR images (Head and others, 1992; Guest and others, 1992; Kreslavsky and Head, 1999). Their stratigraphic significance was recognized in observations in Vellamo Planitia (Aubele, 1994, 1995), which showed that many of the small shield fields represented a regional stratigraphic unit. Subsequently this unit has been recognized in many areas on the planet (Basilevsky and others, 1997; Ivanov and Head, 2001a; Basilevsky and Head, 1998, 2000), including this quadrangle. In association with shield clusters that give the unit a locally hilly texture are isolated outcrops in relatively smooth plains. The shields are interpreted to be of volcanic origin (Aubele and Slyuta, 1990; Guest and others, 1992; Head and others, 1992; Crumpler and Aubele, 2000) and are the likely sources of associated smooth areas. Embayment relations between shield plains and older units are shown in figures 6–10 and those between shield plains and younger units are shown in figures 12 and 16. Although shield plains are typically embayed by the plains with wrinkle ridges and are wrinkle ridged, in some places of the quadrangle, separate shields and even shield clusters are superposed on wrinkle ridges (fig. 11). In the literature, such relatively young shield clusters are sometimes considered as member psh_2 (for example, Basilevsky and Head, 2002b, fig. 12). The psh unit is widely distributed mostly in the southwestern part of the quadrangle and is locally present in its other parts. Its total abundance within V–17 quadrangle is approximately 26 percent, which is significantly larger than the 10 to 15 percent estimates of global occurrence of this unit (Basilevsky and Head, 2000).

Wrinkle ridged plains material (unit pwr, figs. 10, 11, 12, 13, and 14). Next after unit psh is the material of wrinkle-ridged plains. This unit is composed of morphologically smooth, homogeneous plains material of intermediate-low to intermediate-high radar brightness complicated by narrow wrinkle ridges (a structural element). Within the V–17 quadrangle and in other areas of Venus, the wrinkle ridges are typically less than 1 km wide and tens of kilometers long. Locally, however, they may be smaller, whereas in other places they are larger. The unit is interpreted to be plains of volcanic origin deformed by wrinkle ridges (Head and others, 1992; Basilevsky and Head, 1998, 2000). The volcanic (lava) origin of the pwr plains globally and within V–17 is supported by flow-like morphology of one of the members of this unit, although obvious edifices and other sources of these vast lava fields were not observed. Within the V–17 quadrangle is the landing site of the Venera 9 lander (31.01° N., 291.64° E.). Most of the landing ellipse is occupied

by unit pwr so it is very probable that the geochemical analysis suggesting a basaltic composition for the surface material (Surkov, 1997) is characteristic of this unit (Basilevsky and Head, 1998, 2000).

Within V–17 quadrangle, unit pwr is subdivided into three members of different ages (pwr$_1$, pwr$_2$, and pwr$_3$) and in some places where the correspondence of the pwr material to one of these members could not be determined, one more member (pwr$_u$ = undivided) was mapped. Member 1 (pwr$_1$) generally has a relatively low radar albedo (fig. 12). Within the field of member pwr$_1$ at the northeastern flank of the Beta Regio rise there is Omutnitsa Vallis (fig. 13). It is a sinuous, flat-floored groove considered to be a lava channel elsewhere termed "canali" (Baker and others, 1992, 1997). Association of the largest canali of Venus, Baltis Vallis, with member pwr$_1$ was described by Basilevsky and Head (1996). Member 2 (pwr$_2$) generally has a relatively high radar albedo and lobate boundaries indicative of its superposition on pwr$_1$ (fig. 12). Member 3 (pwr$_3$) has been observed only in one locality, northeast of Emegen Corona, where it intrudes into gaps and grabens within member 2 (fig. 14). Its material is relatively radar dark, significantly darker than the pwr$_2$ material and noticeably darker than adjacent areas of member 1. In its dark surface, member pwr$_3$ resembles unit ps, but it differs from unit ps in the presence of wrinkle ridges that form a network in common with wrinkle ridges of the adjacent areas of members pwr$_1$ and pwr$_2$. In several areas of V–17 it was difficult to classify the material of pwr plains into the three members described. It occurred either when the pwr material was darkened to different degrees by haloes of adjacent impact craters or when isolated patches of pwr material were observed among the brighter and typically older units. In these cases it is mapped as member pwr$_u$ (undivided).

Unit pwr occupies approximately 31 percent of the study area, which is significantly smaller than its global abundance (50–60 percent) estimated by Basilevsky and Head (2000). Abundances of the pwr members within V–17 are as follows: pwr$_1$ approximately 11 percent, pwr$_2$, approximately 11 percent, pwr$_3$, approximately 0.2 percent, and pwr$_u$ approximately 9 percent. Plains of unit pwr dominate in the northeastern part of the V–17 quadrangle and form isolated fields among other units in the rest of the study area. Plains with wrinkle ridges and shield plains are often lumped together as "regional plains."

Smooth plains material (unit ps, fig. 15). This is one of the two youngest non-crater material units. Smooth plains material is smooth and radar dark. It is observed in the form of fields of plains 10 to 60 km across, typically of planimetrically irregular outlines, and sometimes rather long tongues of the unit extend to adjacent units. As previously discussed, the ps fields have been called "amoeboids," and described as specific lava flows (Head and others, 1992; Crumpler and Aubele, 2000). Pits about 1 km in diameter are sometimes seen within the ps fields and probably represent volcanic vents. Smooth plains material is usually superposed on unit psh, and in some cases on units pfr, pwr, and tectonic unit fb. Two fields of the ps unit are superposed by ejecta of impact craters Truth and Nalkowska. These craters are also superposed on units psh and pwr and have a faint radar-dark halo. This observation suggests that these two craters, and therefore these two fields of ps material, formed in

the first part of the post-regional-plains time (Basilevsky and Head, 2002a; Basilevsky and others, 2003).

Within the V–17 quadrangle unit ps occupies only approximately 0.15 percent of the area. Basilevsky and Head (2000) did not estimate global abundance of unit ps. They estimated only the combined global abundance (10–15 percent) of units ps and pl (see below). In the V–17 quadrangle, unit ps forms about 20 fields. About half of them are concentrated in the area northeast of Emegen Corona.

Lobate plains material unit (unit pl, fig. 16). The second of the two youngest non-crater material units, lobate plains material, appears morphologically uniform at Magellan SAR resolution. It is mostly radar bright with darker subareas that together form a pattern of superposition of many individual flows. In generally high brightness and flow-like outlines of its fields, unit pl resembles the member pwr$_2$. However the pwr$_2$ fields are usually rather homogeneous in brightness while fields of pl material typically are variegated with a pattern of flow superposition. In addition, the pwr$_2$ fields are wrinkle-ridged whereas the pl fields are not. The prominent flow-like texture and association with obvious volcanic constructs (within V–17 it is Theia Mons) indicate that unit pl is composed of lavas (Head and others, 1992; Crumpler and Aubele, 2000). The Venera 14 landing site, although outside V–17, was located within a field of pl units (Basilevsky and Head, 2000) and X-ray fluorescence analysis of the surface material at the site showed a composition close to tholeiitic basalt (Surkov, 1997). Unit pl embays and is superposed on all other non-crater material units except unit ps with which unit pl is not in contact. Within V–17, unit pl partly floods the 13-km impact crater Raisa and is superposed by the 11-km crater Tako. Both these craters have a faint halo so they are interpreted to have formed within the first half of post-regional-plains time (Basilevsky and Head, 2002a; Basilevsky and others, 2003). Unit pl is locally cut by some young fractures, mostly by those associated with the Devana Chasma rift. Unit pl occupies approximately 5 percent of the V–17 quadrangle. This is about half or smaller than the combined global abundance of units pl and ps estimated by Basilevsky and Head (2000) as 10 to 15 percent. Within V–17 most of unit pl is on the slopes of Theia Mons. A few fields of unit pl 100 to 200 km across are in the northwestern and southeastern parts of the study area and several fields tens kilometers across are observed in other parts of the quadrangle. Among those in the other parts is a volcanic construct, Copacati Mons, about 80 km in diameter and 1 km high centered at 34.8° N., 276.8° E.

Impact crater material (units ci, ch, and cf, figs. 17, 18, and 19). Within the V–17 quadrangle there are 25 impact craters and three splotches (fig. 1, table 1; Schaber and others, 1992, 1998). In most cases it was possible to map separately different facies of crater materials: intra-crater material (ci), hummocky ejecta (ch), and ejecta outflows (cf). In the cases when the crater was small (typically smaller than 6 km in diameter) or it was severely flooded by lavas (the 13-km crater Raisa) undivided crater materials (cu) were mapped. Based on age relations of the crater with regional (psh+pwr) plains and on the degree of crater-associated radar-dark halo (fig. 3), the craters were subdivided into three age facies: a lower one (c$_1$)—pre-regional-plains craters; a middle one (c$_2$)—post-regional-plains craters

with faint or no halo; and an upper one (c_3)—post-regional-plains craters with clear halo. According to Basilevsky and Head (2002a), craters with faint or no halo were formed within the first half of the post-regional-plains time period, while craters with clear haloes—in the second half of this period. Using these two approaches, several combinations were mapped: cu_1, ch_2, cf_3, and so on.

Among the 25 craters of the V–17 quadrangle, one was classified as representing the lower unit c_1 (crater Aigul, fig. 17), twelve as the middle unit c_2 (fig. 18), and twelve as the upper unit c_3 (fig. 19). Splotches, which are radar-dark spots without visible craters inside (Schaber and others, 1992), are similar to the clear crater haloes in their darkness, so they were considered contemporaneous to facies c_3. One crater, Aigul, which is embayed by psh material and classified as of c_1 age, is deformed by the pdf-style fractures and by the faults branching from the fracture belt (fb). The floor of one crater, Deken, superposed on pwr plains and classified as of c_2 age, is deformed by wrinkle ridge whose morphology and orientation are similar to those of wrinkle ridges of the adjacent pwr plains. Four craters (Zvereva, Sanger, Balch, and Olga) are cut by relatively young faults. The fault that cuts crater Zvereva is a part of the radiating system centered at Wohpe Tholus. The faults that cut craters Sanger, Balch, and Olga are structures of the Devana Chasma rift zone. Two of these craters (Zvereva and Sanger) have clear haloes that suggest the tectonic activity responsible for formation of the radiating system centered at Wohpe Tholus as well as Devana Chasma was ongoing in the second half of post-regional-plains time.

Structures

Tectonic Units

Tectonic units are introduced mostly when structures in the study area are spatially very dense and it is difficult or impossible to say what they are deforming. Their identification and mapping were recommended by Wilhelms (1990) and repeated by The Venus Geologic Mappers' Handbook (Tanaka, 1994). Mapping tectonic units allows one not to hypothesize what material units are hidden by this heavy deformation and makes these areas more visible in the map. Three tectonic units have been mapped within the V–17 region: tessera transitional terrain (tt), fracture belts (fb), and rifted terrain (r).

Tessera transitional terrain (unit tt). In the south half of the V–17 quadrangle, extended areas of terrain are observed that resemble tessera in morphology. In a number of localities it is seen that this terrain is formed at the expense of fracturing of the material unit pfr and locally at the expense of the material unit pdf (fig. 20). Some of the fractures in this terrain resemble fractures and faults of tectonic unit r in their variable width (a few hundred meters to 3–4 km), whereas others with less variable width (a few hundred meters) resemble faults of tectonic unit fb. Contrary to units r and fb, this type of terrain forms equidimensional areas within which fractures are typically criss-crossed, rather than planimetric linear zones. In some cases,

when this deformation affects the pfr ridges, the fractures are predominantly transverse to the ridge trends. The typical length of fractures is a few tens of kilometers. Areas with similar morphology have been identified by Ivanov and Head (2001a) as a tectonic unit known as tessera transitional terrain. Accordingly, we mapped these areas as tessera transitional terrain. The morphologic similarity of tt structures to those in the r and pdf tectonic units implies that they are also of extensional origin. Structures of the tectonic unit tt are superposed on broad ridges that typically deform material unit pfr and they do not extend into the neighboring material units psh and pwr. As stated, the precursor terrain for unit tt seems to be the material units pfr and pdf. However, because of the high density of deformation this conclusion is not completely firm. Tectonic unit tt occupies approximately 10 percent of the quadrangle area and composes the southern part of Sudenitsa Tesserae, Zirka Tessera, Hyndla Regio, and a significant part of Rhea Mons. When in contact with the unfractured unit pfr, tessera transitional terrain typically stands a few hundred meters above the adjacent pfr areas.

Fracture belts (unit fb). Within the quadrangle there are linear zones saturated with faults, which themselves are linear, or arcuate, or slightly anastomosing. These faults are typically tens of kilometers long and several hundred meters wide. Their trends are parallel or oblique to the trends of these zones so the faults are often mutually intersecting. These zones have been mapped as a tectonic unit of fracture belts (fig. 21). The fracture belts are considered in the literature as zones of extensional deformation close in origin to the zones of rifted terrain (Hansen and others, 1997; Banerdt and others, 1997; Basilevsky and Head, 2002b). Structures of the tectonic unit fb cut material units t, pdf, and pfr. They are embayed by units psh and pwr but some of the fb faults cut units psh and pwr that distinguish them from the pdf faulting. Lavas of the pl and ps units, when in contact, embay fracture belts and in some cases the fb faults may be the source of small fields of pl lavas. Within the V–17 quadrangle fracture belts occupy approximately 9 percent of the area, being concentrated within the 35 to 40° latitude zone forming Agrona Linea and Shishimora Dorsa. With the Agrona Linea are associated four coronae whose annulae are made of fb unit. Coronae Emegen and Blathnat are part of the Agrona Linea structure. Coronae Rauni and Urash are adjacent to northern periphery of Agrona Linea. In contrast with unit r, the V–17 fracture belts are not associated with topographic troughs. Those associated with the northern base of Beta Regio rise are at the +0.5 to +1.5 altitude range of the topographic slope. Those that make up Dodola Dorsa and Shishimora Dorsa stand a few hundreds meters above the adjacent regional psh+pwr plains.

Rifted terrain (unit r). Long and short linear fractures and sometimes paired and facing scarps interpreted to be grabens are seen in practically all parts of the quadrangle. Their highest concentration is within and nearby Devana Chasma. The places saturated with fractures and grabens have been mapped as a tectonic unit *rifted terrain* (fig. 22). Rift faults are typically several tens of kilometers long, with the longest being 100 to 150 km long. Fractures and grabens of rifted terrain are typically of variable width, and they range from about a hundred meters (limit of resolution) to several kilometers. A

few grabens, including one that cuts the 40-km crater Balch (fig. 3D), are as much as 15- to 20-km wide. Quite often the widths of individual faults are variable. The r fractures and grabens are planimetrically anastomosing and this, together with variability in their width, makes the morphology of this unit very distinctive and recognizable. The r faults deform all material units of the quadrangle including the youngest ps and pl units. Locally the r faults are flooded by pl lavas and this relation is especially typical on Theia Mons. The r faults are likely extensional in origin. Assuming that crater Balch, cut by grabens, was initially planimetrically circular, Solomon and others (1992) estimated that the easterly tectonic extension in this area was about 10 km. The tectonic unit r occupies approximately 2.5 percent of the quadrangle area, mostly in the north-trending axial zone of Beta Regio rise, where it is associated with the Devana Chasma topographic trough, the deepest parts of which are at the +0.5 km to –0.5 km altitude level.

Other Tectonic Features

Several types of tectonic features were observed and mapped within the quadrangle outside the tectonic units. Some of them are considered to be of extensional origin whereas others are contractional. A combination of contractional and extensional structures is typical for tessera-forming deformation. The matrix of tessera terrain in V–17 is ridge-and-groove ensembles, in which ridges and grooves abut each other with practically no horizontal surfaces between them (fig. 6). Ridge-to-ridge or groove-to-groove spacings in these ensembles vary from a few hundred meters to several kilometers with wider features often consisting of clusters of smaller ones. Locally the ridge-and-groove ensembles are cut by flat-bottom grooves with sharp edges and often with obviously late-plains material on their floors. Typically there are two dominant trends of the structures with 60 to 90° angles between them. Sometimes structures criss-cross each other. In other cases, tessera is a complicated mosaic of the 10- to 20-km-blocks within some part of which one trend dominates whereas in other blocks another trend dominates. Locally, structural trends within tessera are noticeably arcuate to almost ring-like (fig. 23). The densely packed ridge-and-groove matrix of tessera terrain probably formed as a result of compressive stresses whereas the flat-floored grooves are grabens (Basilevsky and others, 1986; Bindschadler and Head, 1991; Sukhanov, 1992; Bindschadler and others, 1992a,b; Solomon and others, 1992; Hansen and Willis, 1996; Ivanov and Head, 1996; Hansen and others, 1997).

A specific variety of structures is characteristic of the material unit pdf (fig. 7). They are typically very linear, densely packed, and parallel to each other. In the northeastern part of the V–17 quadrangle, where the pdf unit occupies rather large areas, the unit is a mosaic of subareas. Within each subarea structures are parallel to each other, whereas in different subareas the orientation of the structures is different. The pdf faults are typically several tens of kilometers long and a few hundred meters to 1-km wide. Structures typical of the pdf unit are probably extensional faults, perhaps with involvement of shear.

Contractional structures within the V–17 are represented by ridges of two types. Ridges of the first type form ridge belts but locally single ridges are observed. These ridges usually deform material unit pfr (figs. 9, 10) and locally they deform material unit pdf. An example of when a ridge of this type deforms pdf material can be seen 200 km south of the crater Brooke (fig. 24). The ridges in these belts are the same as those observed and described in other areas of Venus (Frank and Head, 1990; Kryuchkov, 1990; Solomon and others, 1992; Hansen and others, 1997). Ridges are usually 3- to 5-km wide and sometimes as much as 10-km wide and a few tens of kilometers long. The ridge belts of V–17 quadrangle are significantly flooded by the material units psh, pwr, and pl and thus are observed as elongated islands from 100- to 200-km long and 10- to 50-km wide. Within the ridge belts, ridges form clusters with 3- to 15-km ridge-to-ridge spacing whereas some rather extended areas of the pfr unit lack ridges.

The most abundant contractional structures within the V–17 quadrangle are wrinkle ridges that typically deform the material units pwr and psh and locally also observed in unit pfr. The wrinkle ridges are typically a few tens of kilometers long and several hundreds meters wide (figs. 4, 11–14). They usually form networks with ridge-to-ridge spacing varying from 3 to 5 km (typical for member pwr_3 and locally for psh) to 10 to 15 km (typical for subunits pwr_1 and pwr_2). An origin of wrinkle ridges by compressive stress is commonly accepted by many researchers (Pleiscia, 1991; Watters, 1991; Solomon and others, 1992; Banerdt and others, 1997, Bilotti and Suppe, 1997, 1999; Watters and Robinson, 1997). Wrinkle ridges are common on the plains of Venus and the orientation of their networks is indicative of the orientation of stresses that form them. The stress, in turn, may be indicative of the presence of topographic/geoid swells at the time of wrinkle-ridge formation.

Young fractures and grabens cutting practically all material units of the study area are also seen without any direct association with Devana Chasma rift. These faults typically are long (tens to a few hundred kilometers), planimetrically linear or slightly arcuate, with their width being a few hundred meters to 1 km along the fault (fig. 18). These fractures are broadly contemporaneous with the structures of tectonic unit r.

Tectonic History

As a result of geologic mapping several thematic maps have been constructed (figs. 25–32) showing the presence and dominant trends of structures of different ages from tessera-forming deformation to young rift structures. These maps also show the material and tectonic units that host these structures. Also on these maps are shown the +0.5 km and +2.5 km altitude contour lines correspondingly outlining the position of the base and summit of the Beta Regio structural uplift. In cases where structures are numerous, the maps show only a representative part of them. Where structures are short, they were artificially made longer to emphasize their trends.

The major areas occupied by tessera unit and the major tessera-forming structures, are shown in figure 25. Except for a few small localities within the Guinevere Planitia, the largest

of which is seen in the upper right, the tessera areas are concentrated within the Beta Regio uplift. Structural trends, which are mostly outlined by grabens that are part of tessera-forming structures, are rather variegated and show neither consistency within different tessera subareas nor with the planimetric geometry of the Beta Regio rise.

Major areas occupied by densely fractured plains unit (pdf) and the major pdf structures are shown in figure 26. Unlike the areal distribution of tessera unit, the pdf areas are concentrated within Guinevere Planitia and are rare within the Beta Regio rise. The pdf structural trends show a prevalence of northeastern orientations and the partial star-like pattern centered approximately at 41° N., 288° E. (fig. 26). No correlation is observed between the pdf structural trends and the planimetric geometry of the Beta Regio rise.

The major areas occupied by ridged and fractured plains unit (pfr), and the relatively broad ridges deforming it, are shown in figure 27. Clusters of these broad ridges form the ridge belts. The map shows that most pfr localities are within the Beta Regio rise and east of it within Hyndla Regio. With the exception of the ridges of Iyele Dorsa in northern V–17 and their continuation to the south, which both trend north, the majority of ridge belts and single ridges show a slightly variable northwest orientation. No correlation of the ridge and ridge belt trends with the Beta Regio rise geometry was observed.

The major areas occupied by tessera transitional terrain (tt) and the fractures deforming them are shown in figure 28. The map shows that the tt localities are concentrated within the Beta Regio rise, Hyndla Regio, and Zirka Tessera, mostly in spatial association with areas occupied by the pfr unit. Major trends of the tt fractures are often transverse to the trends of the ridge belts, but some structures show different trends. No correlation of tt fracture trends and the Beta Regio rise geometry was observed.

The areas occupied by fracture belts (fb) and major trends of the fb structures are shown in figure 29. A significant part of the fb tectonic unit approximately follows the +0.5 km contour line. This contour roughly outlines the northern boundary of the Beta Regio topographic rise; this relation underscores the correlation of the fracture belts in this part of V–17 and the planimetric geometry of the Beta Regio rise. To the east, the fracture belt trend changes its orientation so that it becomes perpendicular to the base of the Beta Regio rise. Another cluster of fb structures approximately perpendicular to the base of Beta Regio is in the northwestern part of the quadrangle (Dodola Dorsa). The fb structures outline all four coronae of the quadrangle: Rauni, Urash, Emegen, and Blathnat. The fb structures are also part of the radiating structures centered at Wohpe Tholus.

The areas occupied by wrinkle-ridged regional plains (psh + pwr) and the major trends of wrinkle ridges are shown in figure 30. As noted, the psh unit crops out mostly within the Beta Regio rise, whereas the pwr unit is widespread outside Beta Regio. Orientation of trends of wrinkle ridges varies significantly within the quadrangle. North of Beta Regio the region within the Guinevera Planitia wrinkle-ridge trends show some parallelism with the orientation of the base of northern Beta Regio. But in other places they show no obvious relation with the planimetric geometry of the Beta Regio rise: along

with orientations being parallel to the Beta Regio outlines, there are similar numbers of orientations normal and oblique to them. In this respect Beta Regio rise differs significantly from several large topographic rises (for example, Western Eistla) around which the wrinkle-ridge networks show an alignment parallel to the rise boundaries (Basilevsky, 1994; Bilotti and Suppe, 1999).

Areas occupied by the rifted terrain tectonic unit (r) and major post-regional-plains faults are shown in figure 31. Shown also are areas occupied by the post-regional-plains units ps and pl. The map shows that unit r is in the northeast axial zone of the Beta Regio rise and that the faults feathering from unit r zone show northwestern and northeastern trends radiating to the north from Rhea and Theia Montes. This observation suggests that both rifting and the Beta Regio uplift are parts of the same process. In the northern part of the quadrangle a significant number of the young (post-regional-plains) faults radiate around Wohpe Tholus. Within the quadrangle there are also young faults that show no obvious association with either the Beta Regio uplift or with the radiating feature centered at Wohpe Tholus, but they are not abundant. In the areas where the young pl and ps lavas were observed, young faults are often present. This is especially typical for Theia Mons. However, young faults of Rhea Mons and most other areas show little if any association with young lavas.

Individual types of structures shown in figures 25 to 31 are combined in figure 32. This figure shows that the V–17 area is dominated by the Beta Regio uplift in the structural sense. It is very prominent in topography and is more than +5 km above the neighboring Guinevere Planitia. In its structural pattern the Beta Regio uplift is outlined by the Devana Chasma rift zone and by the fracture belts of Agrona Linea around its northern base.

Other structures of the area are significantly smaller than the Beta Regio uplift. Figure 32 shows several centers of radiating fractures, all mapped earlier by Ernst and others (2003). The most prominent are the following four, centered at 34.5° N., 293.5° E.; 39° N., 277° E.; 40° N., 279.5° E., 42° N., 287.5° E. The first three of these are part of the fracture belt. The fourth one, is centered at Wohpe Tholus, is composed of several generations of structures. Its northeast and southeast sectors have abundant faults associated with pdf. Its southwest sector is partly made of structures associated with fb. Young, post-regional-plains structures radiate in almost all directions.

Swarms of ridge belts trending mostly northwest and going through the Beta Regio uplift with no alignment with it, as well as swarms of wrinkle ridges, are also shown in figure 33. The wrinkle ridges are mostly of variable orientations, except at the very northern part of V–17, where south-to-southwest trends dominate. Trends of tt, pdf, and t structures are present in relatively small windows, and they appear rather variable with almost no orientation heritage with time.

Geologic History

Eight material units, two of which are subdivided, and three tectonic units were identified and mapped. These material units and structural units r and fb are essentially the same as units identified and mapped by other researchers in other

regions of Venus. Structural unit tt earlier identified by Ivanov and Head (2001a) was mapped here for the first time. Although other researchers often used unit names different from the V–17 names, the inter-region (inter-quadrangle) unit correlations are not difficult (see summary of the unit inter-region correlations in Basilevsky and Head, 2000). A unique aspect of the V–17 region is the presence within it of three different members of plains with wrinkle ridges (pwr$_1$, pwr$_2$, and pwr$_3$). In most other regions of Venus there are only two members correlative to our pwr$_1$ and pwr$_2$ (see for example, Basilevsky and Head, 2000). In some subareas, however, for the reasons described above, correspondence of the observed pwr material with either of these subunits could not be found, so the fourth subunit was introduced: undivided pwr material (pwr$_u$).

Among the impact crater materials (c), three subunits of different ages (c$_1$, c$_2$, and c$_3$) have been distinguished. This was accomplished based on the degree of degradation of the crater-related radar-dark haloes (Basilevsky and Head, 2002a; Basilevsky and others, 2003) and using the analyses of age relations between craters and other units and structures. This approach provided the possibility to date semi-quantitatively several geologic events of the region. For example, the crater Deken (fig. 18) has a faint associated radar halo, which suggests it formed within the first half of the post-regional-plains time period. Southwest of the crater its ejecta outflow buries an adjacent graben and is also cut by another graben, both of which radiate from the stellate structure (astrum) centered at Wohpe Tholus. These relations suggest that at least part of these faults formed during this time interval. Another fault that is part of this structure cuts the crater Zvereva, which has an associated prominent dark halo. The observation that this fault cuts crater Zvereva implies that faulting forming this astrum continued into the second half of the post-regional-plains time. Deformation of the ejecta outflow of the crater Sanger (which has a prominent radar-dark halo) by faults branching from the Devana Chasma rift suggests that rifting activity occurred during the second part of post-regional-plains time.

The general time sequence of units mapped within V–17 is the same as in other regions of the planet, with tessera material (t) at the bottom of the stratigraphic column and materials of the lobate (pl) and smooth (ps) plains at the top. The abundance of some units and structures as well as the presence of the Beta Regio topographic rise are what make the V–17 quadrangle different from many other regions of Venus. Within the V–17 quadrangle, the abundance of unit pwr (approximately 31 percent) is about half the global abundance of this unit, whereas abundance of unit psh (approximately 26 percent) is about twice the global abundance (Basilevsky and Head, 2000). Within V–17, the tectonic unit tt, tessera transitional terrain (approximately 10 percent), is abundant, whereas in the regions mapped by Ivanov and Head (2001a) it is rather rare. Similarly, tectonic unit fb (approximately 9 percent) is characterized by an abundance 2 to 3 times greater than its global abundance (Basilevsky and Head, 2000). The presence of the Beta Regio structural uplift reflects the activity of a large mantle plume, which is responsible not only for the topographic rise but also for Theia Mons pl volcanism and the localization of the Devana Chasma rift as well as the Agrona Linea fracture belts.

Summarized in the following paragraphs are the results of the geologic analysis and mapping with emphasis on the geologic history. Tessera material (t), the oldest material unit of the area, is so heavily deformed by tectonism that its litho-logic/petrologic nature can not be morphologically recognized. The morphology of tessera terrain within V–17, as elsewhere, implies intensive contractional and extensional deformation (see for example, Barsukov and others, 1986; Basilevsky and others, 1986; Bindschadler and Head, 1991; Bindschadler and others, 1992b; Ivanov and Head, 1996; Hansen and Willis, 1996; Gilmore and others, 1997). Structural trends of tessera-forming deformation are variegated, suggesting local rather than regional control of geometry of stresses responsible for deformation. The major areas where tessera terrain is observed are in the southern part of V–17, but smaller islands of tessera are also seen in the north among the younger units (fig. 25). These observations suggest that tessera material may be present everywhere in the quadrangle underlying the younger material units.

Next in time sequence is the material of densely fractures plains (pdf). If one removes the fracturing, the unit represents a plains-forming material. This was the basis on which Basi-levsky and Head (1998, 2000) suggested that the pdf material was primarily mafic lavas. The fracturing in pdf is dense, prob-ably extensional, and may also be characterized by local shear. Fracturing is subparallel within areas tens of kilometers across, and changes orientations within the largest outcrops that are 100 to 300 km across. This observed change in orientation, as in the case of tessera-forming deformation, suggests local rather than regional control of geometry of stresses responsible for defor-mation. The structural pattern of the pdf unit is different from that of the t unit and this difference implies a significant change in deformation style. Major areas where the pdf unit is observed are concentrated in the northwestern part of the V–17 quadran-gle. Smaller outliers of the unit are seen, however, in other areas of the quadrangle (fig. 26), so one may infer that the densely fractured plains material is rather widespread in the quadrangle underlying the younger material units.

The next-youngest unit, material of fractured and ridged plains (pfr), is typically deformed by broad contractional ridges that form ridge belts. This deformation is modest, so there is no doubt that the unit consists of a plains-forming material. Ignor-ing differences in deformation styles, the pfr and pwr materials appear very much the same, and this similarity was the basis for Basilevsky and Head (1998, 2000) to suggest that these units are basaltic lavas. Trends of ridges in pfr, although variable, show a certain consistency, suggesting regional rather than local control of geometry of stresses responsible for deformation. On the basis of these relationships, it appears that since the time of pdf fracturing, the deformation style changed significantly: wide-spread but locally controlled extensional deformation changed into widespread but regionally controlled contractional defor-mation. The ridge belts of V–17 show no alignment with the planimetric geometry of the Beta Regio topographic rise. This observation implies that at the time of ridge formation the Beta Regio topographic rise either did not yet exist, or was not yet high enough to produce topographic stresses affecting the trends of ridge belts. The pfr unit is more abundant in the southern half of V–17, but its small islands are also seen among the younger

plains in the north (fig. 27). It is inferred that the fractured and ridges plains material is rather widespread in the quadrangle, especially in its northern part, where it underlies the younger material units.

Following pfr ridging there were two deformational episodes: extensional fracturing that transformed large areas of the pfr unit into tessera transitional terrain (tt) and extensional fracturing that formed the fracture belts (fb). The first episode appears to be at least partly earlier than the second one. In rare cases where the tt unit is in contact with fb (in the eastern part of the quadrangle), fb faults cut the tt unit. The tt unit is embayed by psh+pwr regional plains. Although the fb unit is embayed by these plains, some fb unit faults cut into the plains. The tt structural pattern implies little or no predominant stress orientation (fig. 28), whereas the fb structures are organized in prominent linear belts locally complicated with concentric patterns. The concentric patterns outline the four coronae mapped within the V–17 quadrangle. A significant number of fb structures are in alignment with northern base of the Beta Regio rise (fig. 29). The tt structural pattern shows no alignment with the Beta Regio rise geometry.

Next in time was the emplacement of the shield plains unit (psh). The unit morphology suggests that it was formed when mafic lavas erupted from numerous spatially scattered edifices (Head and others, 1992). Compared to pfr-forming volcanism, which primarily produced morphologically smooth plains, the psh eruption style is quite different. Shield plains are typically wrinkle ridged but the wrinkle ridge network is usually a part of the pwr plains emplaced later. Within the V–17 quadrangle, the major areas of the psh unit are within the Beta Regio rise and are associated with fracture belts and densely fractured plains. The psh plains typically underlie the younger pwr, pl, and ps units but it is not clear how widespread the unit is beneath them. The abundance of the psh unit within V–17 is about twice its global abundance. Ivanov and Head (2001a) interpreted this relationship to mean that the Beta Regio rise had reached sufficient elevation by the end of the time of emplacement of unit psh so lavas of unit pwr-flooded lows around the regional high, preferentially preserving the earlier psh unit. Alternatively, it may be at least partly due to more favorable thermal environment for the formation of the shield fields within the Beta Regio rise and fracture belts.

The younger member of the psh+pwr suite, plains with wrinkle ridges (pwr), consists of three members that form a stratigraphic sequence: pwr_1, pwr_2, and pwr_3. Unit pwr_1 is composed of the relatively dark primarily smooth material (fig. 12), and it is considered part of the volcanic plains (see Head and others, 1992). Its volcanic nature is inferred on the basis of its smooth plains-like surface and embayment relations, although it has no visible eruption sources or flow-like features except the Omutnitsa Vallis channel (fig. 13), which belongs to category of features interpreted to be formed by lava flow and thermal erosion (Baker and others, 1992, 1997). The volcanic origin of the suite of pwr members is strengthened by the morphology of unit pwr_2, which forms extensive relatively radar bright flows (fig. 12). Unit pwr_3 consists of relatively radar dark material and, as with unit pwr_1, does not show obvious morphologic evidence of volcanic sources and features. The abundance

of the pwr_1 and pwr_2 members is about the same (approximately 10.5 percent), but keeping in mind that subunit pwr_2 is almost certainly underlain by subunit pwr_1, one can conclude that areas influenced by volcanic floods during emplacement of unit pwr_2 became significantly smaller compared to emplacement of unit pwr_1. The very small area of subunit pwr_3 appears to continue this trend.

Unit pwr is deformed by wrinkle ridges whose networks form topography on the psh+pwr suite that is embayed and overlain by the younger units pl and ps. Wrinkle ridges were formed as a result of modest contractional deformation (Plescia, 1991; Watters, 1991; Solomon and others, 1992; Banerdt and others, 1997, Bilotti and Suppe, 1997, 1999; Watters and Robinson, 1997). Within the V–17 quadrangle they form a single network that deforms the psh unit and the pwr members with no evidence of different generations of ridges separated by the material (members) units. The orientation of wrinkle ridges within the V–17 quadrangle is generally not in alignment with the planimetric geometry of the Beta Regio rise. This observation implies that at the time of wrinkle ridging, the Beta Regio topographic rise either did not exist, or it was not high enough to produce topographic stress sufficient to influence the trends of ridge belts. The second option looks preferable because the fracture belts that formed earlier than the wrinkle ridges already show alignment with northern base of the Beta Regio rise.

Emplacement of the suite of smooth (ps) and lobate (pl) plains was next in time. The morphology of both of these material units suggests that they were formed from eruption of mafic lavas (see Head and others, 1992). In the case of the smooth plains these were eruptions of small volumes of very liquid lavas penetrating into narrow faults and gaps. This type of volcanism seems to be a continuation of the volcanic style typical of subunit pwr_3. Eruptions of lavas that form lobate plains are mostly associated with the Theia Mons volcano. These were voluminous eruptions that formed rather extended fields of relatively radar-bright lavas. This partly resembles the volcanic style typical of subunit pwr_2. A few fields of unit ps are superposed by the impact craters Truth and Nalkovska, which have faint radar-dark haloes. This characteristic implies that these lava fields were emplaced within the first half of post-regional-plains time. A similar age constraint is seen for the lobate plains lavas, superposed by the ejecta of the crater Tako, which has a faint associated halo. These observations, however, do not exclude the possibility that pl and ps volcanism continued into the second half of the post-regional-plains time.

Following the episode of contractional wrinkle ridging, and generally contemporaneous with the emplacement of units pl and ps within the mapped area, there was a phase of extensional tectonism probably extending up to the present time. During this phase, the Devana Chasma rift zone and the linear extensional faults not directly related to the rift were formed. The Devana Chasma rift zone coincides with the north-trending axis of the Beta Regio rise, which suggests the rise and the rift formed as part of a single process. No observations suggest how soon the rifting started after the wrinkle ridging phase. Deformation of the ejecta outflow of the clear-halo crater Sanger by faults feathering from the Devana Chasma rift, however, suggests

13

that the rift was active at least for some time within the second part of the post-regional-plains period. Results of geophysical modeling suggest that the Beta Regio uplift continues today (see Leftwich and others 1999; Vezolainen and others, 2003, 2004).

Within the V–17 quadrangle there are 25 impact craters. One of them, Aigul, formed prior to the emplacement of the shield plains and perhaps even earlier, before the dense fracturing of pdf material. The remaining 24 craters are superposed on the regional plains and the younger units. Based on the degree of preservation of crater-associated radar-dark haloes, one can conclude that twelve craters were formed within the first half of the post-regional-plains time, and that the remaining twelve craters were formed within the second half of this time period. Three splotches identified within the quadrangle appear as dark as the clear halo associated with the twelve younger craters and are probably of the same age.

In summary, with the exception of impact crater materials, the material units of this area are primarily composed of mafic lavas. For material of densely fractured plains, this statement is mostly a hypothesis, but for units pfr and pwr$_1$ it is very probable and for all other units it is obvious. The style of the volcanism changed with time. It is not possible to say anything certain about the volcanism that formed material of the densely fractured plains, except that it was probably plains-forming. Judging from the similarities described of the pfr and pwr$_1$ materials, one can conclude that the first was emplaced in vast plains-forming lava floods. This was followed by a phase of volcanism of very different style: fields of relatively small volcanic shields. Then, with some overlap, there was again a phase of vast lava floods. During emplacement of unit pwr$_2$, the areal extent of the plains-forming floods shrank, and it became even more localized during emplacement of unit pwr$_3$. The subsequent suite of lobate and smooth plains formed generally simultaneously with each other, but the styles of volcanism that formed them were different; often extensive lobate flows formed the lobate plains and very low shields formed small smooth fields, correspondingly.

By subdividing sequences of lavas into mappable units and unit suites as well as assessing their relationships to structures, the nature of deformational phases and their intensity can be assessed. The intensity of deformation obviously decreased with time, from very intensive tessera- and pdf-forming deformation to moderately intensive deformation that formed ridge belts and tt-faulting on unit pfr, and then the wrinkle ridge network on the suite of psh+pwr units plains. During the post-regional-plains time, there was a lack of globally distributed deformation. Deformational belts within the quadrangle can be traced subsequent to post-pfr time, first fracture belts and then the Devana Chasma rift zone with its branches. Rare but extensive linear faults formed during the post-regional-plains time, part of them as late as the activity associated with astrum centered at Wohpe Tholus.

The large-scale topography of the mapped area since the emplacement of the densely fractured plains probably consisted of two components: hilly plains in the north and relatively low uplands to the south. The signatures of development of the Beta Regio uplift in the southern part of the quadrangle are distinguishable since post-pfr time (fracture belts of the Beta north base), but significant growth of the Beta Regio rise occurred during the post-regional-plains time and perhaps it is ongoing.

Acknowledgements

References Cited

Alexandrov, Yu.N., Crymov, A.A., Kotelnikov, V.A., Petrov, G.M., Rzhiga, O.N., Sidorenko, A.I., Sinilo, V.P., Zakharov, A.I., Frim, E.L., Basilevsky, A.T., Kadnichansky, S.A., and Tyuflin, Yu.S., 1986, Venus—Detailed mapping of Maxwell Montes region: Science, v. 231, p. 1271–1273.

American Commission on Stratigraphic Nomenclature, 1961, Code of Stratigraphic Nomenclature: American Association of Petroleum Geologists Bulletin, v. 45, no. 5, p. 645–665.

Arvidson, R.E., Greeley, R.M., Malin, C., Saunders, R.S., Izenberg, N., Plautt, J.J., Wall, S.D., and Weitz, C.M., 1992, Surface modification of Venus as inferred from Magellan observations of plains: Journal of Geophysical Research, v. 97, p. 13,303–13,317.

Aubele, J.C., 1994, Stratigraphy of small volcanoes and plains terrain in Vellamo Planitia, Venus [abs.], in Lunar and Planetary Science Conference, 25th, March 14–18, 1994: Houston, Texas, Lunar and Planetary Institute, p. 45–46.

Aubele, J.C., 1995, Stratigraphy of small volcanoes and plains terrain in Vellamo Planitia-Shimti Tessera region, Venus [abs.]: Lunar and Planetary Science Conference, 26th, March 13–17, 1994, Houston, Texas, Lunar and Planetary Institute, p. 59–60.

Aubele, J.C., and Slyuta, E.N., 1990, Small domes on Venus— Characteristics and origin: Earth, Moon, and Planets, v. 50/51, p. 493–532.

Baker, V.R., Komatsu, G., Gulick, V.C., and Parker, T.J., 1997, Channels and valleys, in Bougher, S.W., Hunten, D.M., and Phillips, R.J., eds., Venus II geology, geophysics, atmosphere, and solar wind environment: Tucson, University of Arizona Press, p. 757–793.

Baker, V.R., Komatsu, G., Parker, T.J., Gulick, V.C., Kargel, J.S., and Lewis, J.S., 1992, Channels and valleys on Venus—Preliminary analysis of Magellan data: Journal of Geophysical Research, v. 97, p. 13,421–13,444.

Banerdt, W.B., McGill, G.G., and Zuber, M.T., 1997, Plains tectonics on Venus, in Bougher, S.W., Hunten, D.M., and Phillips, R.J., eds., Venus II geology, geophysics, atmo-

sphere, and solar wind environment: Tucson, University of Arizona Press, p. 901–930.

Barsukov, V.L., Basilevsky, A.T., and 28 others, 1986, The geology and geomorphology of the Venus surface as revealed by the radar images obtained by Venera 15 and 16: Proceedings of Lunar and Planetary Science Conference, 16th, Journal of Geophysical Research, v. 96, no. B4, p. D378–D398.

Barsukov, V.L., Basilevsky A.T., Pronin, A.A., and 20 others, 1984, First results of geologic-morphologic analysis of radar images of Venus surface taken by the Venera 15/16 probes: The USSR Academy Doklady, v. 279, no 4, p. 946–950. (In Russian).

Basilevsky A.T., 1988, Northern Beta: Photogeologic analysis of Venera 15/16 images and maps [abs.], in Lunar and Planetary Science Conference, 19th, Lunar and Planetary Institute, Houston, Texas, March 14–18, 1988, Abstracts, p. 41–42.

Basilevsky, A.T., 1994, Concentric wrinkle ridge pattern around Sif and Gula [abs.]: Lunar and Planetary Science Conference, 25th, March 14–18, 1994, Houston, Texas, Lunar and Planetary Institute, p. 63–64.

Basilevsky, A.T., and Head, J.W., 1995a, Global stratigraphy of Venus—Analysis of a random sample of thirty-six test areas: Earth, Moon, and Planets, v. 66, p. 285–336.

Basilevsky, A.T., and Head, J.W., 1995b, Regional and global stratigraphy of Venus—A preliminary assessment and implications for the geologic history of Venus: Planetary and Space Science, v. 43, p. 1,523–1,553.

Basilevsky, A.T., and Head, J.W., 1996, Evidence for rapid and widespread emplacement of volcanic plains on Venus—Stratigraphic studies in the Baltis Vallis region: Geophysical Research Letters, v. 23, p. 1,497–1,500.

Basilevsky, A.T., and Head, J.W., 1998, The geologic history of Venus—A stratigraphic view: Journal of Geophysical Research, v. 103, no. E4, p. 8,531–8,544.

Basilevsky, A.T., and Head, J.W., 2000, Geologic units on Venus—Evidence for their global correlation: Planetary and Space Science, v. 48, p. 75–111.

Basilevsky, A.T., and Head, J.W., 2002a, Venus—Analysis of the degree of impact crater deposit degradation and assessment of its use for dating geological units and features: Journal of Geophysical Research, v. 107, no. E8, doi: 10.1029/2001JE001584.

Basilevsky, A.T., and Head, J.W., 2002b, On rates and styles of late volcanism and rifting on Venus: Journal of Geophysical Research, v. 107, no. E6, doi: 10.1029/2000JE001471, p. 8-1-8-17.

Basilevsky, A.T., Head, J.W., Schaber, G.G., and Strom, R.G., 1997, The resurfacing history of Venus, in Bougher, S.W., Hunten, D.M., and Phillips, R.J., eds., Venus II geology, geophysics, atmosphere, and solar wind environment: Tucson, University of Arizona Press, p. 1,047–1,084.

Basilevsky, A.T., Head, J.W., and Setyaeva, I.V., 2003, Venus—Estimation of age of impact craters on the basis of degree of preservation of associated radar-dark deposits: Geophysical Research Letters, v. 30, no. 18, p. 1950, doi:1029.2003GL017504.

Basilevsky, A.T., Pronin, A.A., Ronca, L.B., Kryuchkov, V.P., Sukhanov, A.L., and Markov, M.S., 1986, Styles of tectonic deformations on Venus—Analysis of Venera 15 and 16 data: Proceedings of Lunar and Planetary Science Conference 16th, Journal of Geophysical Research, v. 91, p. D399–D411.

Bender, K.C., Senske, D.A., and Greeley, R., 2000, Geologic map of the Carson Quadrangle (V–43), Venus, U.S. Geological Survey Geologic Investigations Series Map I–2813, scale 1:5,000,000.

Bilotti, F., and Suppe, J., 1997, Wrinkle ridges and the tectonic history of Venus [abs.]: Lunar and Planetary Science Conference, 28th, March 17–21, 1997, Houston, Texas, Lunar and Planetary Institute, abstract #1630, [CD-ROM].

Bilotti, F., and Suppe, J., 1999, The global distribution of wrinkle ridges on Venus: Icarus, v. 139, p. 137–157.

Bindschadler, D.L., and Head, J.W., 1991, Tessera terrain, Venus—Characterization and models for origin and evolution: Journal of Geophysical Research, v. 96, p. 5,889–5,907.

Bindschadler, D.L., Kreslavsky, M.A., Ivanov, M.A., Head, J.W., Basilevsky, A.T., and Shkuratov, Yu.G., 1990, Distribution of tessera terrain on Venus—Prediction for Magellan: Geophysycal Research Letters, v. 17, p. 171–174.

Bindschadler, D., Schubert, D., and Kaula, W.M., 1992a, Coldspots and hotspots—Global tectonics and mantle dynamics of Venus: Journal of Geophysical Research, v. 97, p. 13,495–13,532.

Bindschadler, D.L., Decharon, A., Beratan, K.K., Smrekar, S.E., and Head, J.W., 1992b, Magellan observations of Alpha Regio—Implications for formation of complex ridged terrains on Venus: Journal of Geophysical Research, v. 97, p. 13,563–13,578.

Brian, A.W., Stofan, E.R., and Guest, J.E., 2005, Geologic map of the Taussig Quadrangle (V–39), Venus, U.S. Geological Survey Geologic Investigations Series Map I–2813, scale 1:5,000,000.

Bridges, N., and McGill, G.E., 2002, Geologic Map of the Kaiwan Fluctus Quadrangle (V–44), Venus: U.S. Geological Survey Geologic Investigations Series Map I–2747, scale 1:5,000,000.

Campbell, B.A., 1995, Use and presentation of Magellan quantitative data in Venus mapping: U.S. Geological Survey Open-File Report 95–519, 32 p.

Campbell, B.A., and Campbell, P.G., 2002, Geologic map of the Bell Regio Quadrangle (V–9), Venus, U.S. Geological Survey Geologic Investigations Series Map I–2743, scale 1:5,000,000.

Campbell, D.B., Head, J.W., Harmon, J.K., and Hine, N.N., 1984, Venus—Volcanism and rift formation in Beta Regio: Science, v. 226, p. 167–170.

Crumpler, L.S., Aubele, J.C., Senske, D.A., Keddie, S.T., Magee, K.P., and Head, J.W., 1997, Volcanoes and centers of volcanism on Venus, in Bougher, S.W., Hunten, D.M., and Phillips, R.J., eds., Venus II geology, geophysics, atmosphere, and solar wind environment: Tucson, University of Arizona Press, p. 697–756.

15

Crumpler, L.S., and Aubele, J.C., 2000, Volcanism on Venus, in Encyclopedia of volcanoes: San Diego, London, Academic Press, p. 727–770.

DeShon, H.R., Young, D.A., and Hansen, V.L., 2000, Geologic evolution of southern Rusalka Planitia, Venus: Journal of Geophysical Research, v. 105, no. E3, p. 6,983–6,996.

Elachi, C., 1987, Introduction to the physics and techniques of remote sensing: New York, Wiley and Sons, 413 p.

Ernst, R.E., Desnoyers, D.W., Head, J.W., and Grosfils, E.B., 2003, Graben fissure systems in Guinevere Planitia and Beta Regio (264°–312° E., 24°–60° N.), Venus and implications for regional stratigraphy and mantle plumes: Icarus, v. 164, p. 282–316.

Florensky C.P., Ronca L.B., Basilevsky A.T., Burba G.A., Nikolaeva O.V., Pronin A.A., Trakhtman A.M., Volkov V.P., and Zasetsky V.V., 1977, The surface of Venus as revealed by Soviet Venera 9 and 10: Geological Society of America Bulletin, v. 88, no 11, p. 1537–1545.

Ford, P.G., and Pettengill, G.H., 1992, Venus topography and kilometer-scale slopes: Journal of Geophysical Research, v. 97, p. 13,102–13,114.

Foster, A., and Nimmo, F., 1996, Comparisons between the rift systems of East Africa, Earth, and Beta Regio, Venus: Earth and Planetary Science Letters, v. 143, p. 183–195.

Frank, S.L., and Head, J.W., 1990, Ridge belts on Venus—Morphology and origin: Earth, Moon, and Planets, v. 50/51, p. 421–470.

Gilmore, M.S., Ivanov, M.A., Head, J.W., and Basilevsky, A.T., 1997, Duration of tessera deformation on Venus: Journal of Geophysical Research, v. 102, p. 13,357–13,368.

Goldstein, R.M., 1965, Preliminary Venus radar results: Journal of Research of National Bureau of Standards, Section D, no. 69D, p. 1,623–1,625.

Goldstein, R.M., 1967, Radar studies of Venus, in Dolfus, A., ed., Moon and Planets: North-Holland, Amsterdam, p. 126–131.

Goldstein, R.M., and Rumsey, H.C., 1972, A radar image of Venus: Icarus, v. 17, p. 699–703.

Goldstein, R.M., Green, R.R., and Rumsey, H.C., 1978, Venus radar brightness and altitude images: Icarus, v. 36, p. 334–352.

Greeley, R., Bender, K.C., Saunders, R.S., Schubert, and Weitz, C.M., 1997, Aeolian processes and features on Venus, in Bougher, S.W., Hunten, D.M., and Phillips, R.J., eds., Venus II geology, geophysics, atmosphere, and solar wind environment: Tucson, University of Arizona Press, p. 547–589.

Guest, J.E., Bulmer, M.H., Aubele, J., Beratan, K., Greeley, R., Head, J.W., Michaels, G., Weitz, C., and Wiles, C., 1992, Small volcanic edifices and volcanism in the plains of Venus: Journal of Geophysical Research, v. 97, p. 15,949–15,966.

Hansen, V.L., 2000, Geologic mapping of tectonic planets: Earth and Planetary Science Letters, v. 176, p. 527–542.

Hansen, V.L., and DeShon, H.R., 2002, Geologic map of the Diana Chasma Quadrangle (V–37), Venus, U.S. Geological Survey Geological Investigations Series Map I–2752, scale 1:5,000,000.

Hansen, V.L., and Willis, J.J., 1996, Structural analysis of a sampling of tesserae—Implications for Venus geodynamics: Icarus, v. 123, p. 296–312.

Hansen, V.L., Willis, J.J., and Banerdt, W.B., 1997, Tectonic overview and synthesis, in Bougher, S.W., Hunten, D.M., and Phillips, R.J., eds., Venus II geology, geophysics, atmosphere, and solar wind environment: Tucson, University of Arizona Press, p. 797–844.

Head, J.W., Crumpler, L.S., Aubele, J.C., Guest, J. E., and Saunders, R. S., 1992, Venus volcanism: Classification of volcanic features and structures, associations, and global distribution from Magellan data: Journal of Geophysical Research, v. 97, p. 13,153–13,197.

Herrick, R.R., and Phillips, R.J., 1992, Geologic correlations with the interior density structure of Venus: Journal of Geophysical Research, v. 97, p. 16,017–16,034.

Herrick, R.R., and Phillips, R.J., 1994, Implications of a global survey of Venusian impact craters: Icarus, v. 111, no. 2, p. 387–416.

Ivanov, M.A., 2001, Morphology of the tessera terrain on Venus—Implications for the composition of tessera material: Solar System Research, v. 35, no. 2, p. 1–17.

Ivanov, M.A., and Head, J.W., 1996, Tessera terrain on Venus— A survey of the global distribution, characteristics, and relation to surrounding units: Journal of Geophysical Research, v. 101, p. 14,861–14,908.

Ivanov, M.A., and Head, J.W., 2001a, Geology of Venus: mapping of a global geotraverse at 30° N latitude: Journal of Geophysical Research, v. 106, p. 17,515–17,566.

Ivanov, M.A., and Head, J.W., 2001b, Geologic map of the Lavinia Planitia Quadrangle (V–55), Venus: U.S. Geological Survey Geologic Investigations Series Map I–2684, scale 1:5,000,000.

Ivanov, M.A., and Head, J.W., 2004. Geologic map of the Atalanta Planitia (V–4) quadrangle, Venus: U.S. Geological Survey Geologic Investigations Series Map I–2792, scale 1:5,000,000.

Keldysh, M.V., ed., 1979, First panoramas of Venus surface: Moscow, Nauka Press, 132 p. (in Russian).

Klose, K.B., Wood, J.A., and Hashimoto, A., 1992, Mineral equilibria and the high radar reflectivity of Venus mounttops: Journal of Geophysical Research, v. 97, p. 16,353–16,369.

Konopliv, A.S., and Sjogren, W.L., 1994, Venus spherical harmonic gravity model to degree and order 60: Icarus, v. 112, p. 42-54.

Konopliv, A.S., Banerdt, W.B., and Sjogren, W.L., 1999, Venus gravity: 180th degree and order model: Icarus, v.139, p. 3–18.

Kotelnikov, V.A., Yashchenko, V.R., Zolotov, A.F., and 14 other co-editors, 1989, Atlas of Venus Surface, The Main Department of Geodesy and Cartography. The USSR Council of Ministers, Moscow, 329 p. (in Russian).

Kreslavskii, M.A., Bazilevskii, A.T., and Shkuratov, Yu.G., 1988, Prognosis of the distribution of the tessera terrain on Venus using PV and Venera 15/16 data: Solar System Research, v. 24, no 4, p. 173–182.

Kreslavsky, M.A., and Head, J.W., 1999, Morphometry of small

shield volcanoes on Venus: Implication for the thickness of regional plains: Journal of Geophysical Research, v. 104, p.18,925–18,932.

Kryuchkov, V.P., 1990, Ridge belts—Are they compressional or extensional structures?: Earth, Moon, and Planets, v. 50–51, p. 471–491.

Leftwich, T.E., von Frese, R.R.B., Kim, H.R., Potts, L.V., Roman, D.R., and Tan, L, 1999, Crustal analysis of Venus from Magellan satellite observations at Atalanta Planitia, Beta Regio, and Thetis Regio: Journal of Geophysical Research, v. 104, p. 8,441–8,462.

Mackwell, S.J., Zimmerman, M.E., Kohlstedt, D.L., and Scherber, D.S., 1995, Experimantal deformation of dry Colombia diabase—Implications for tectonics of Venus, *in* Daemon, J.J.K., and Schultz, R.A., eds: Rock mechanics, Proceedings of the 35th U.S. Symposium. Rotterdam, Germany, Balkema, p. 207–214.

Mackwell, S.J., Zimmerman, M.E., and Kohlstedt, D.L., 1998, High temperature deformation of dry diabase with implications to tectonics on Venus: Journal of Geophysical Research, v. 103, p. 975–984.

Malin, M.C., 1992, Mass movements on Venus: Preliminary results from Magellan cycle 1 observations: Journal of Geophysical Research, v. 97, p. 16,337–16,352.

Masursky, H., Eliason, E., Ford, P.G., McGill, G.E., Pettengill, G.H., Schaber, G.G., and Schubert, G., 1980, Pioneer-Venus radar results—Geology from the images and altimetry: Journal of Geophysical Research, v. 85, p. 8,232–8,260.

McGill, G.E., Steenstrup, S.J., Barnon, C., and Ford, P.G., 1981, Continental rifting and the origin of Beta Regio, Venus: Geophysycal Research Letters, v. 8, p. 737–740.

McKinnon, W.B., Zahnle, K.J., Ivanov, B.A., and Melosh, H.J., 1997, Cratering on Venus—Models and observations *in* Bougher, S.W., Hunten, D.M., and Phillips, R.J., eds., Venus II geology, geophysics, atmosphere, and solar wind environment: Tucson, University of Arizona Press, p. 969–1014.

Moroz, V.I, and Basilevsky, A.T., 2003, Venus missions, *in* Mark, Hans, ed., Encyclopedia of space science and technology: Hoboken, NJ, John Wiley and Sons, p. 841–857.

Phillips, R.J., Grim, R.E., and Malin, M.C., 1991, Hot-spot evolution and the global tectonics of Venus: Science, v. 252, p. 651–658.

Phillips, R.J., and Malin, M.C., 1983, The interior of Venus and tectonic implications, *in* Hunten, D.M., Colin, L., Donahue, T.M., and Moroz, V.I., eds., Venus: Tucson, University of Arizona Press, p. 159–214.

Plescia, J.B., 1991, Wrinkle ridges in Lunae Planum, Mars—Implication for shortening and strain: Geophysical Research Letters, v. 18, p. 913–916.

Rathbun, J.A., Janes, D.M., and Squyres, S.W., 1999, Formation of Beta Regio, Venus—Results from measuring strain: Journal of Geophysical Research, v. 104, p. 1,917–1,927.

Rosenberg, E., and McGill, G.E., 2001, Geologic Map of the Pandrosos Dorsa Quadrangle (V–5), Venus: U.S. Geological Survey Geological Investigations Series Map I–2721, scale 1:5,000,000.

Saunders, R.S., Spear, A.J., Allin, P.C. and 24 others, 1992, Magellan mission summary: Journal of Geophysical Research, v. 97, p. 13,067–13,090.

Schaber, G.G., 1982, Venus—Limited extension and volcanism along zones of lithospheric thickness: Geophysical Research Letters, v. 9, p. 499–502.

Schaber, G.G., Strom, R.G., Moore, H.J., Soderblom, L.A., Kirk, R.L., Chadwick, D.J., Dawson, D.D., Gaddis, L.R., Boyce, J.M., and Russell, J., 1992, Geology and distribution of impact craters on Venus—What are they telling us?: Journal of Geophysical Research, v. 97, p. 13,257–13,302.

Schaber, G.G., Kirk, R.L., and Strom, R.G., 1998, Data base of impact craters on Venus based on analysis of Magellan radar images and altimetry data: U.S. Geological Survey Open-File Report 98–104.

Senske, D.A., Schaber, G.G., and Stofan, E.R., 1992, Regional topographic rises on Venus: Geology of western Eistla Regio and comparison to Beta Regio and Atla Regio: Journal of Geophysical Research, v. 97, p. 13,395–13,420.

Smrekar, S.E., Kiefer, W.S., Stofan, E.R., 1997, Large volcanic rises on Venus, in Bougher, S.W., Hunten, D.M., and Phillips, R.J., eds., Venus II geology, geophysics, atmosphere, and solar wind environment: Tucson, University of Arizona Press, p. 845–878.

Solomatov, V.S., and Moresi, L.N., 1996, Stagnant lid convection on Venus: Journal of Geophysical Research, v. 101, p. 4,737–4,754.

Solomon, S.C., Smrekar, S.E., Bindschadler, D.L., Grimm, R.E., Kaula, W.M., McGill, G.E., Phillips, R.J., Saunders, R.S., Schubert, G., Squyres, S.W., and Stofan, E.R., 1992, Venus tectonics: An overview of Magellan observations: Journal of Geophysical Research, v. 97, p. 13,199–13,256.

Squyres, S.W., Jankowski, D.G., Simons, M., Solomon, S.C., Hager, B.H., and McGill, G.E., 1992, Plains tectonism on Venus—The deformation belts of Atalanta Planitia: Journal of Geophysical Research, v. 97, p. 13,579–13,600.

Stofan, E.R., Guest, J.E., 2003. Geologic Map of the Aino Planitia Quadrangle (V–46), Venus: U.S. Geological Survey Geologic Investigations Series Map I–2779, scale 1:5,000,000.

Stofan, E.R., Head, J.W., Campbell, D.B., Zisk, S.H., Bogomolov A.F., Rzhiga O.N, Basilevsky, and Armand, N.A., 1989, Geology of a rift zone on Venus: Beta Regio and Devana Chasma: Geological Society of America Bulletin, v. 101, p. 143–156.

Sukhanov, A.L., 1992, Tesserae, *in* Barsukov, V.L., Basilevsky, A.T., Volkov, V.P., and Zharkov, V.N., eds., Venus geology, geochemistry, and geophysics: Tucson, University of Arizona Press, p. 82–95.

Sukhanov A.L., Pronin A.A., Burba G.A., Nikishin A.M., Kryuchkov V.P., Basilevsky A.T., Markov M.S., Kuzmin R.O., Bobina N.N., Shashkina V.P., Slyuta E.N., and Chernaya I.M., 1989, Geomorphic/geologic map of part of the northern hemisphere of Venus, *in* Batson, R.M., Basilevsky, A.T., Burba, G.A., Head, J.W., coordinators, Atlas of Venus, 1:15,000,000 topographic series: U.S. Geological Survey Geologic Investigations Series Map I–2059.

Surkov, Yu.A., 1997, Exploration of terrestrial planets from spacecraft—Instrumentation, investigation, and interpretation, (2d ed.), Hoboken, N.J., John Wiley, 446 p.

Surkov, Yu.A., Kirnozov, F.F., Glazov, V.N., and others, 1976, Contents of natural radioactive elements in Venusian rocks based on data of the Venera 9 and 10 probes: Kosmicheskie Issledovaniya, v. 14, no. 5, p. 781–785.

Tanaka, K.L. (compiler), 1994, Venus geologic mappers' handbook, (2d ed.): U.S. Geological Survey Open-File Report 94–438, 50 p.

Tyler, G.L., Simpson, R.A., Maurer, M.J., and Holmann, E., 1992, Scattering properties of the Venusian surface—Preliminary results from Magellan: Journal of Geophysical Research, v. 97, p. 13,115–13,140.

Vezolainen, A.V., Solomatov, V.S., Head, J.W., Basilevsky, A.T., and Moresi, L.-N., 2003, Timing of formation of Beta Regio and its geodynamical implications: Journal of Geophysical Research, v. 108, no. E15002, doi:10.1029/2002JE001889.

Vezolainen, A.V., Solomatov, V.S., Basilevsky, A.T., and Head, J.W., 2004, Uplift of Beta Regio—Three-dimensional models: Journal of Geophysical Research, v. 109, no. E08007, doi:10.1029/2004JE002259.

Watters, T.R., 1991, Origin of periodically spaced wrinkle ridges on the Tharsis Plateau of Mars: Journal of Geophysical Research, v. 96, p. 15,599–15,616.

Watters, T.R., and Robinson, M. S., 1997, Radar and photoclinometric studies of wrinkle ridges on Mars: Journal of Geophysical Research, v. 102, p. 10,899–10,903.

Wilhelms, D.E., 1990, Geologic mapping, in Greeley, R. and Batson R.M., eds., Planetary mapping: New York, Cambridge University Press, p. 208–260.
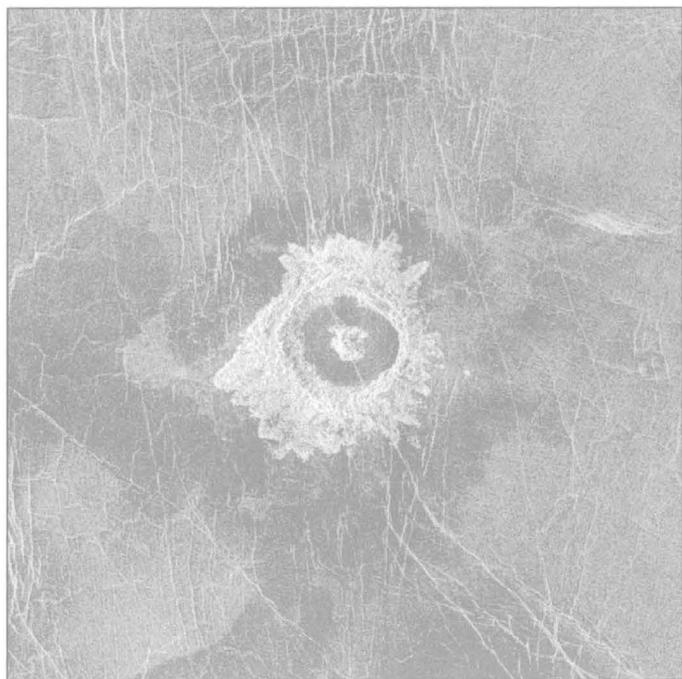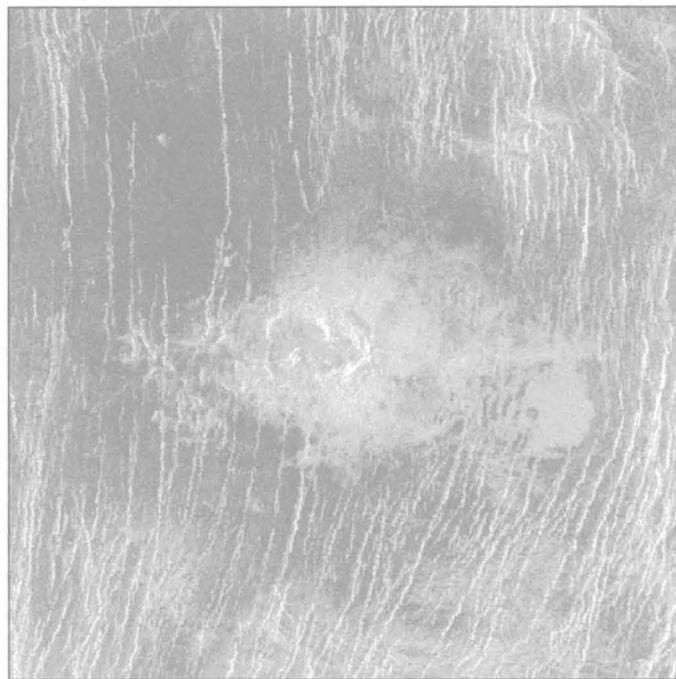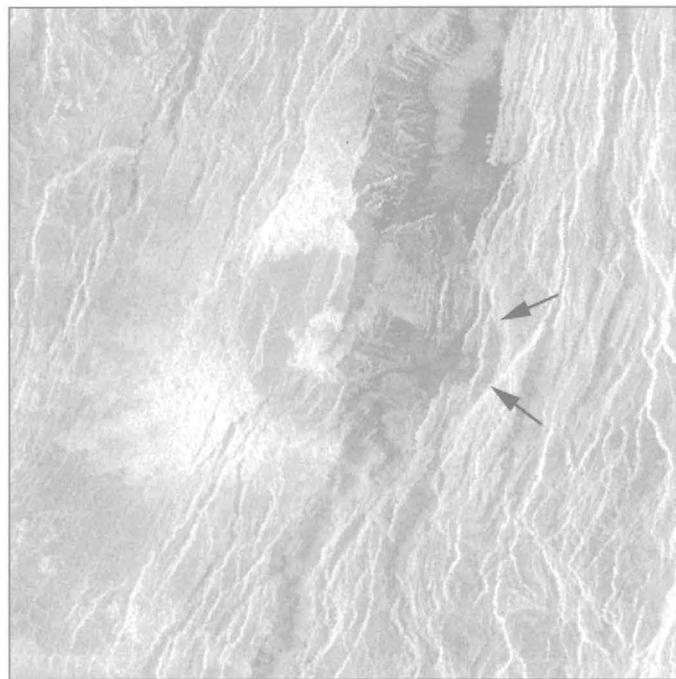
Figure 3. Examples of impact craters in the Beta Regio quadrangle: *A*, The crater Zvereva (D (diameter) = 22.9 km, 45.36° N., 283.12° E.) with a clear radar-dark halo and a radar-bright hummocky ejecta; *B*, The crater Daphne (D = 15.5 km, 41.3° N., 280.4° E.) with a clear radar-dark halo and medium-bright ejecta outflows; *C*, The crater Wazata (D = 13.9 km, 33.6° N., 298.3° E.) with a faint halo; *D*, The crater Balch (D = 40 km, 29.9° N., 282.9° E.) with no halo. The crater Balch is cut by grabens of the Devana Chasma rift. Sizes of images are about 115 by 115 km for figure parts *A*, *B*, and *D*, and 70 by 70 km for figure part *C*.
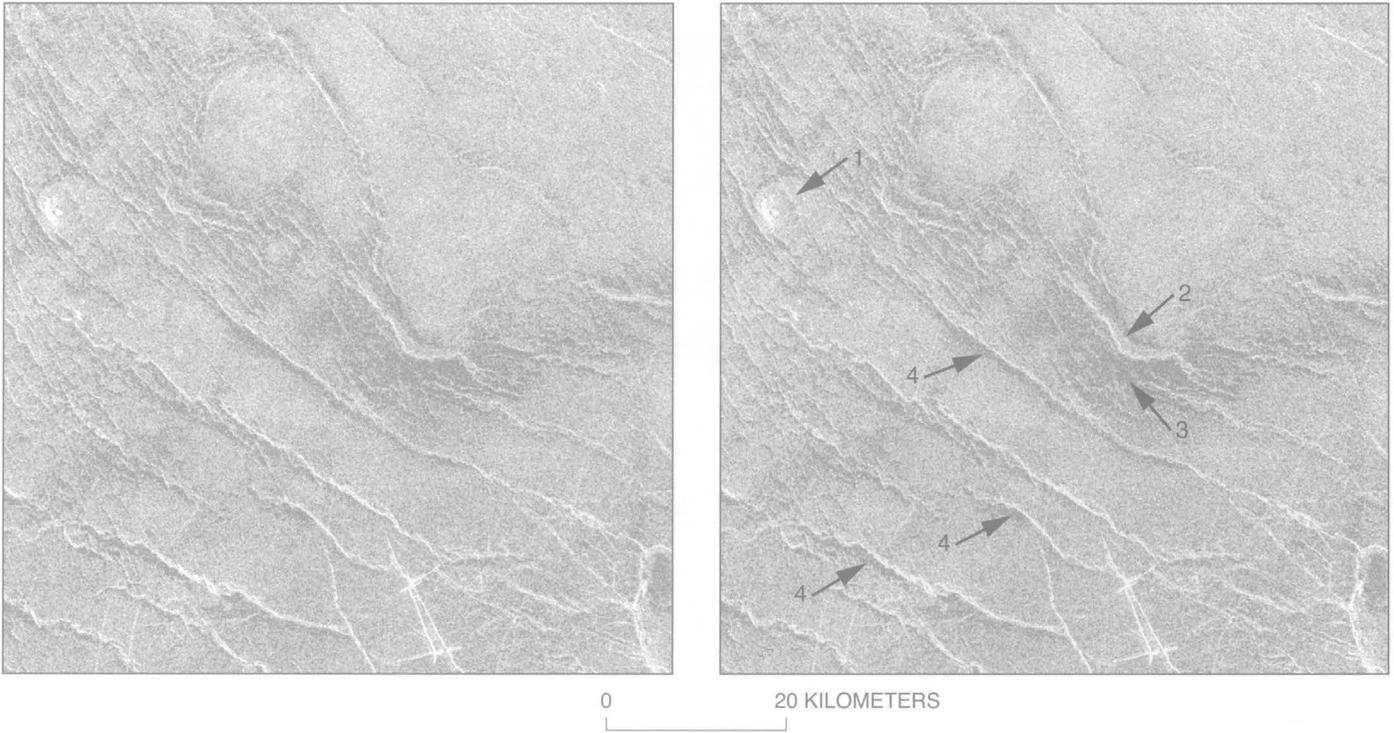
Figure 4. Area of plains with wrinkle ridges on the northeastern flank of Beta Regio topographic rise. This left-looking image, centered at 32° N., 295° E., shows a small volcanic shield (1) and wrinkle ridges (2), both illuminated from the left. Near a prominent wrinkle (marked 2) there is a radar-dark mantle with diffuse boundaries (marked 3). Accumulations of radar-dark material are also seen at the western base of several wrinkle ridges (marked 4). Size of image is about 70 by 70 km.

Magellan

0   20 KILOMETERS

Venera 9

Figure 5. Signatures of downslope mass movement. *Top*: Part of Magellan F-Map image, centered at 30.4°
N., 283.3° E., showing the western slope of the north-trending graben (white arrows mark upper edge of the
slope) with downslope trending grooves in the upper part of the slope and accumulations of relatively bright
material (talus?) in the lower part of it. *Bottom*: Part of the TV panorama taken by the Venera 9 lander.
Decimeter-sized rock fragments are on the steep slope dipping towards the image top. The T-shaped device
in the lower right is 40 cm across.
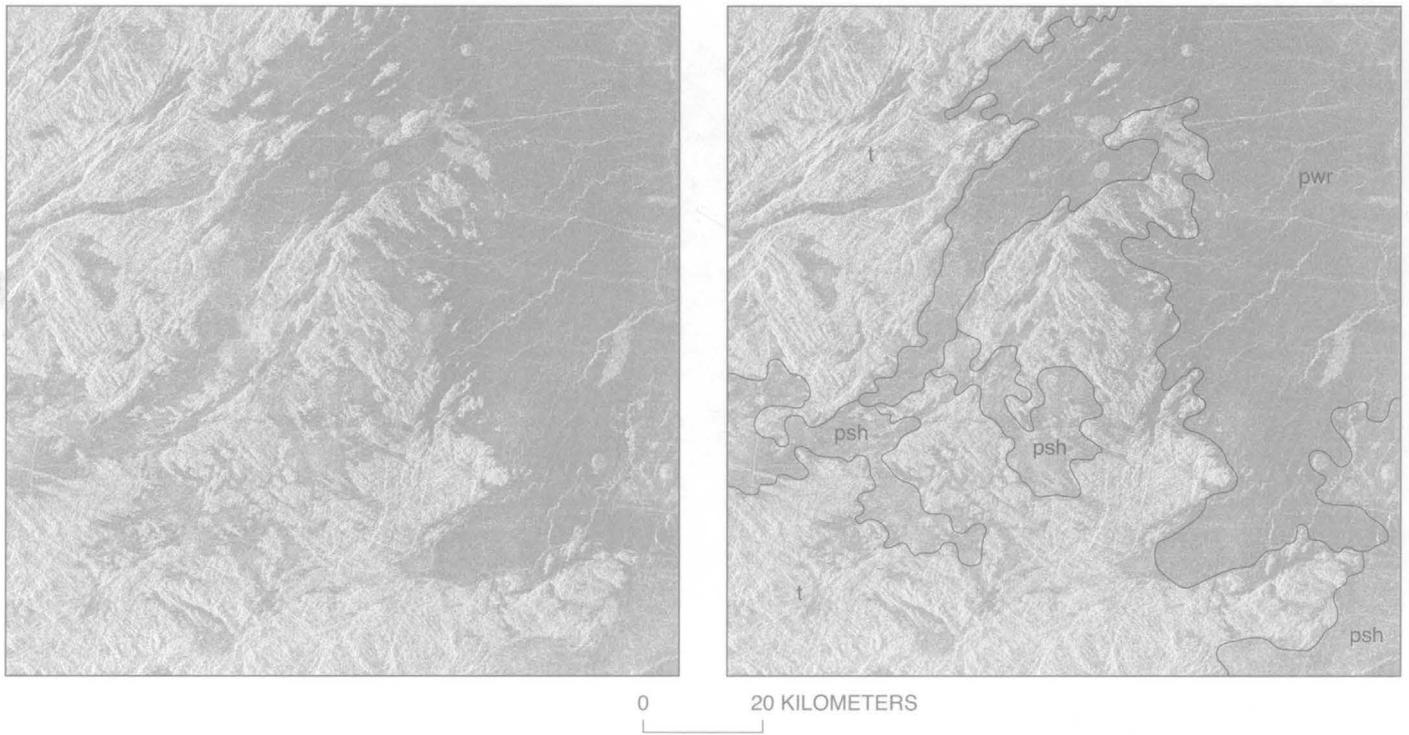
Figure 6. Area of tessera terrain (t) embayed by shield plains (psh) and plains with wrinkle ridges (pwr). Image centered at 34.5° N., 275.5° E. Size of image is about 105 by 105 km.
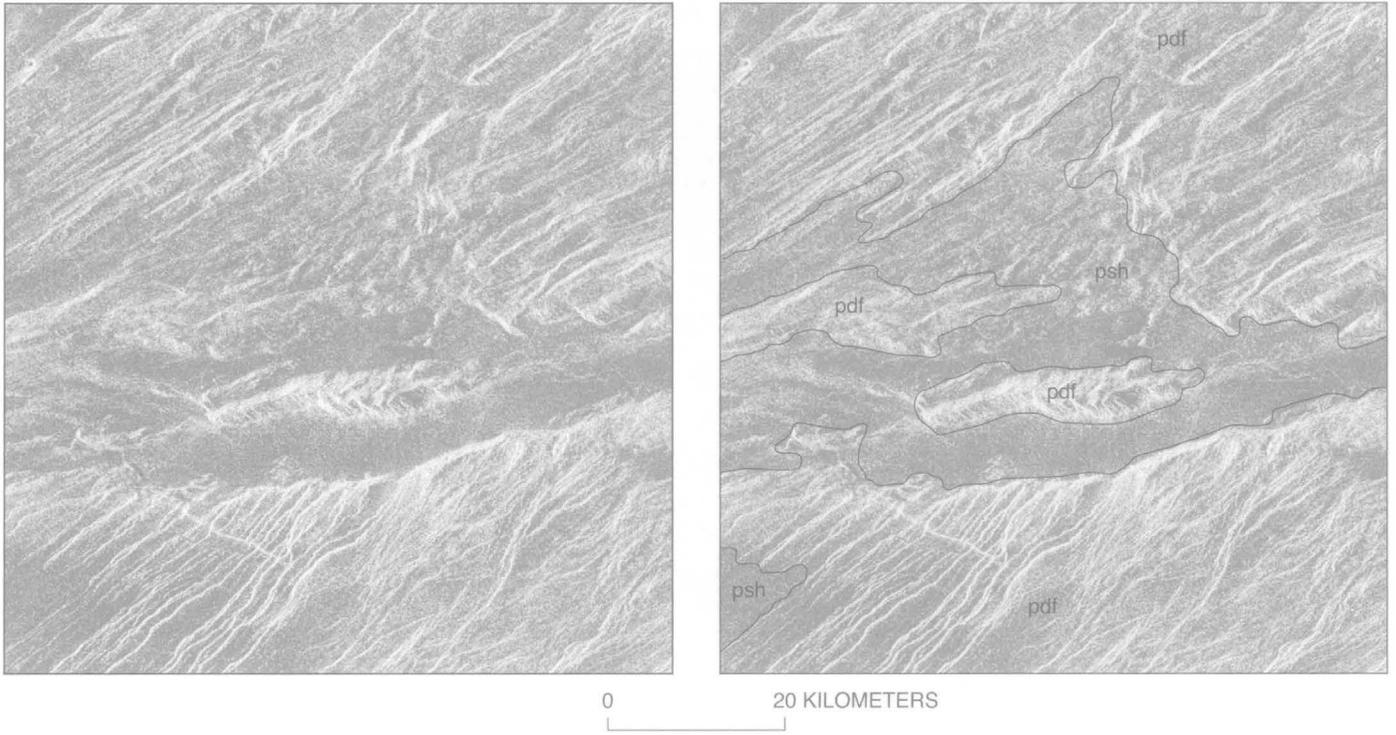
Figure 7. Densely fractured plains (pdf) locally embayed by shield plains (psh). This image is centered at 42.3° N., 291.5° E. and is part of Lachesis Tessera, which contrary to its name consists mostly of the unit pdf, not tessera terrain. Image centered at 42.4° N., 298.5° E. Size of image is about 75 by 75 km.
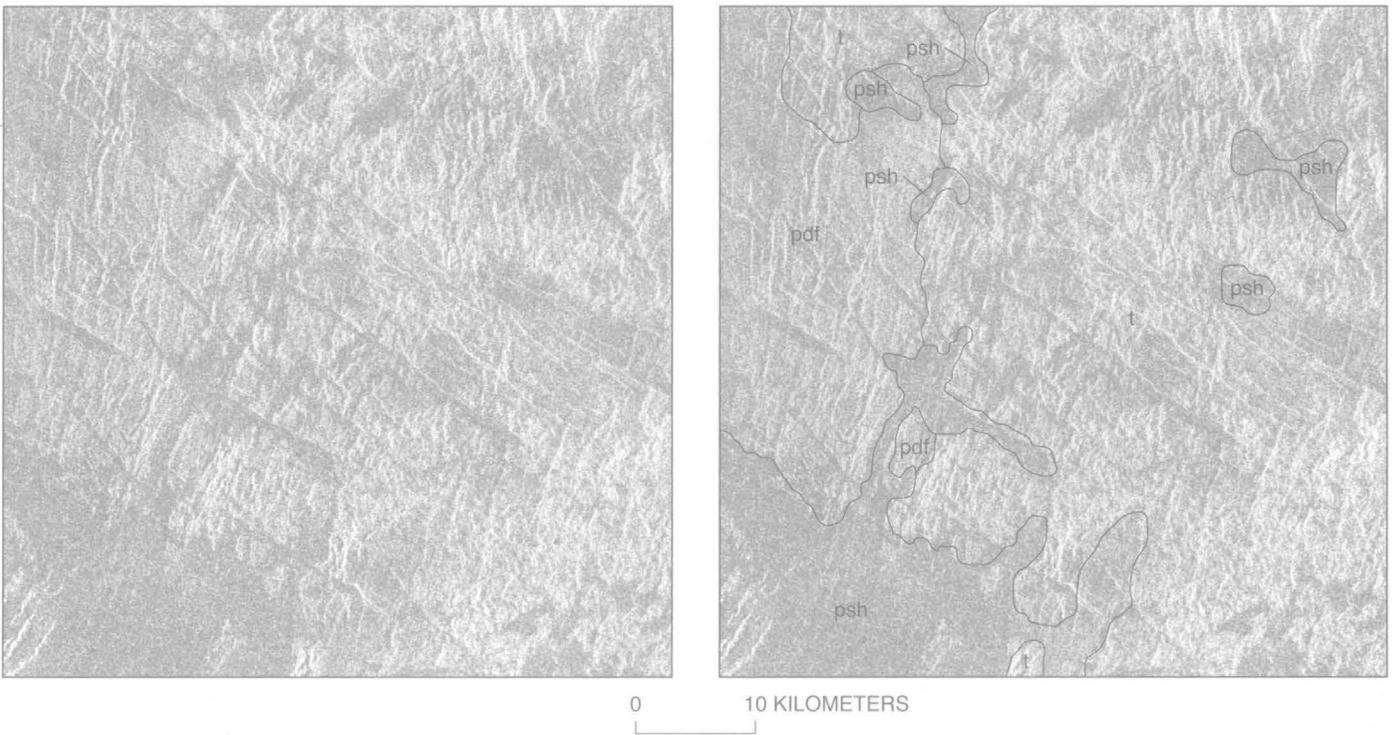
Figure 8. Densely fractured plains (pdf) that embay tessera terrain (t). Tessera is dominated by two transversal sets of structures whereas unit pdf is dominated by only one set; this distinction makes it possible to draw a boundary between them. Both pdf and t units are locally embayed by the shield plains (psh). Image centered at 44.2° N., 294.4° E. Size of image is about 55 by 55 km.
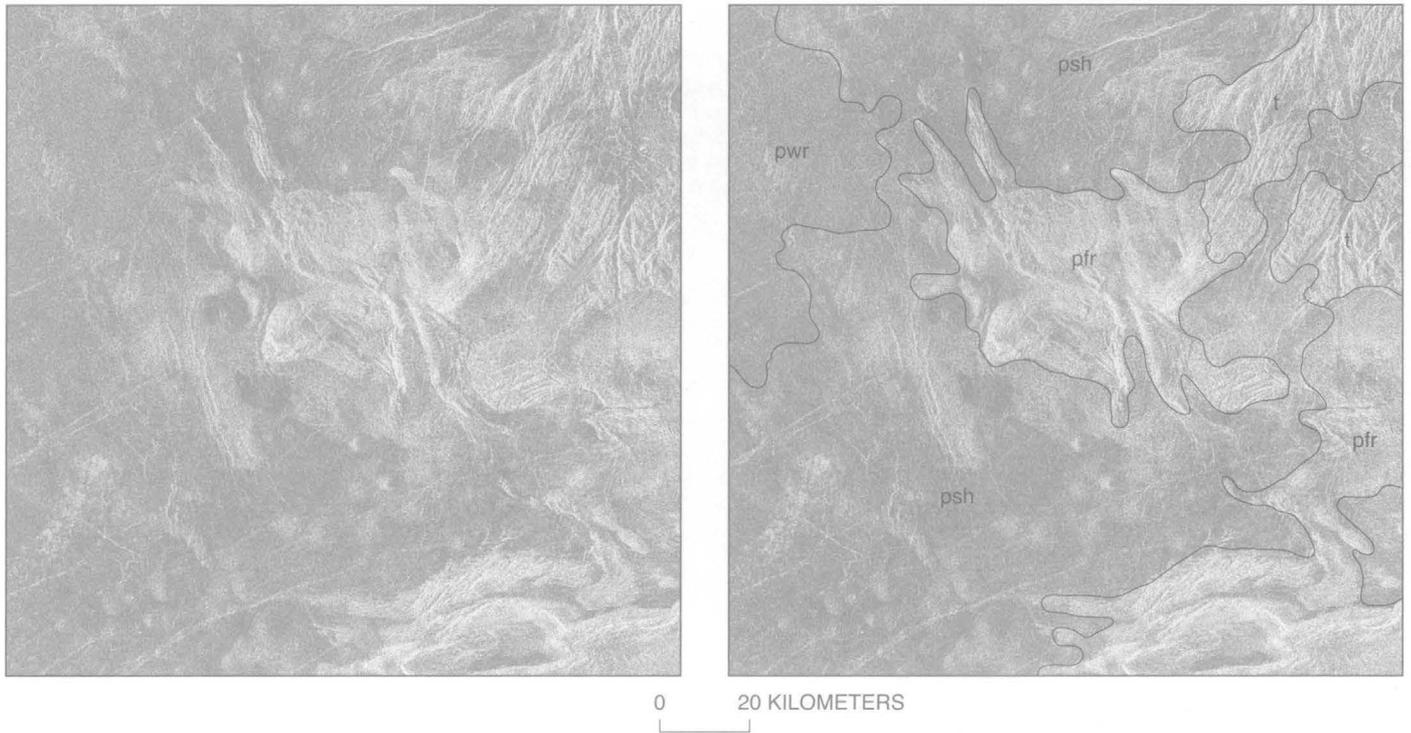
Figure 9. Fractured and ridged plains (pfr) embayed by shield plains (psh) and embaying tessera terrain (t). Tessera structures do not extend into unit pfr. Unit pfr is deformed by relatively broad (3–5 km) ridges. Image centered at 30.1° N., 272.4° E. Size of image is about 145 by 145 km.
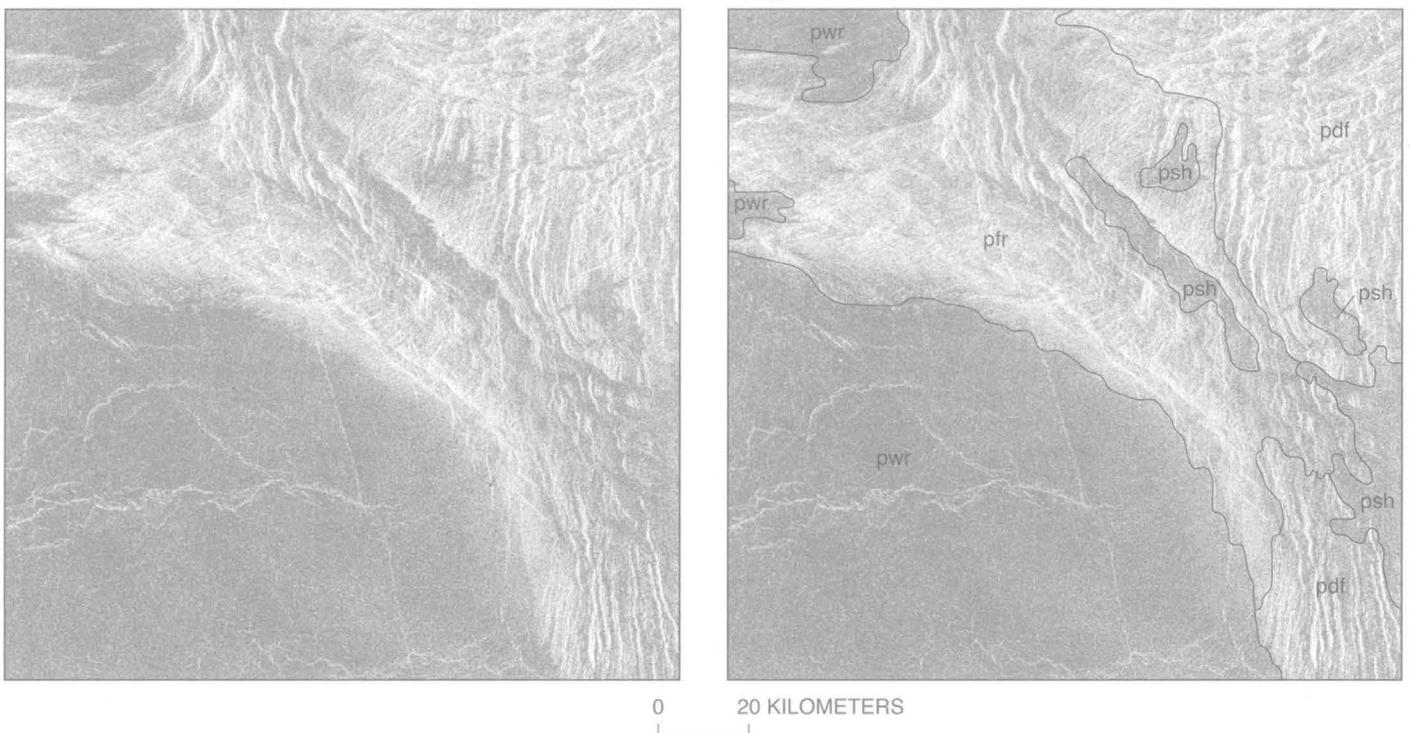
Figure 10. Fractured and ridged plains (pfr) embaying densely fractured plains (pdf). Both pfr and pdf units are embayed by pwr and psh materials. Image centered at 49.6° N., 294.2° E. Size of image is about 145 by 145 km.
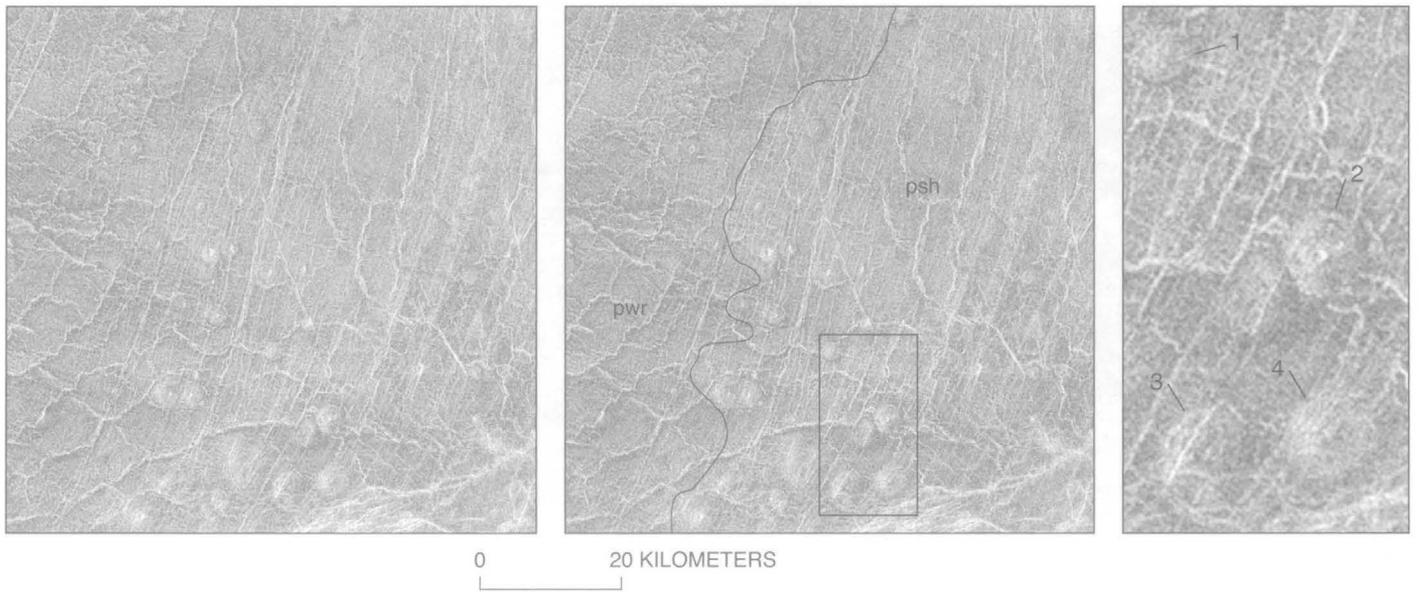
Figure 11. Shield plains (psh) and pwr plains on the northeastern flank of Beta Regio rise. The right figure shows an enlargement of part of the image with shields superposed on wrinkle ridges (labeled 1 and 2) and deformed by wrinkle ridges (labeled 3 and 4). Image centered at 32.8° N., 292.9° E.
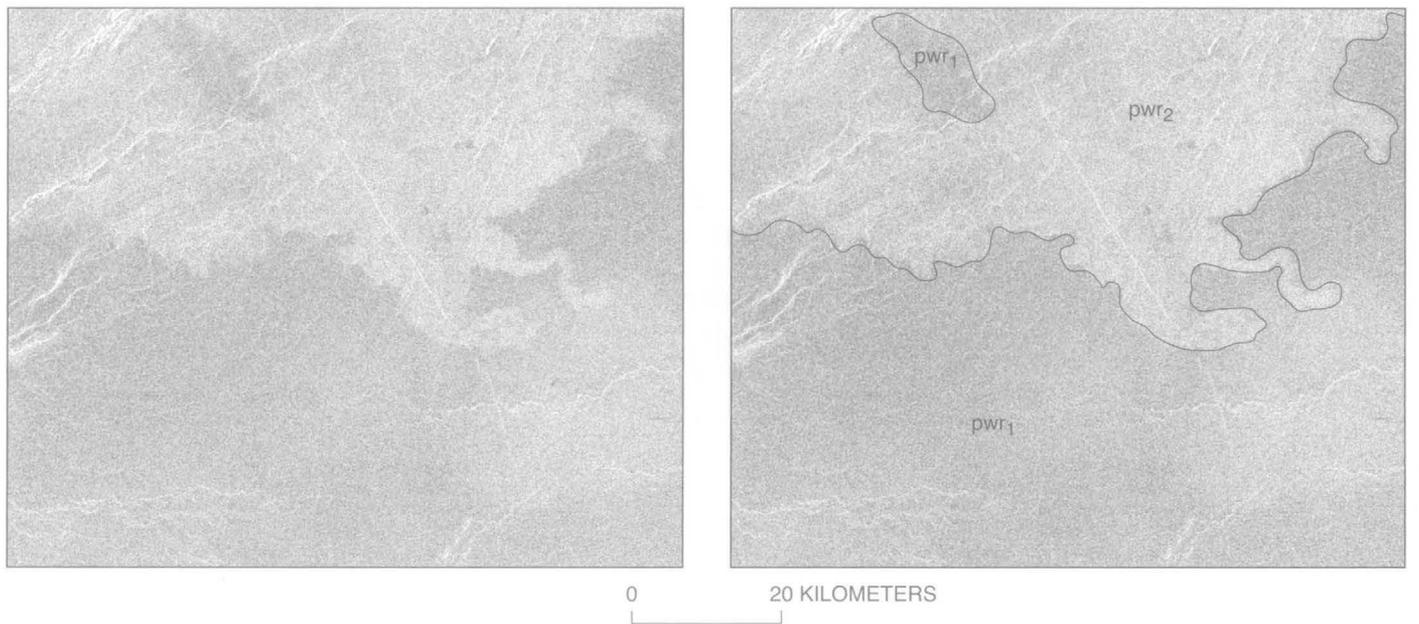
Figure 12. Member 1 (pwr_1) and member 2 (pwr_2) of plains with wrinkle ridges of Guinevere Planitia. Image centered at 48.1° N., 282.9° E. Size of image is about 75 by 75 km.
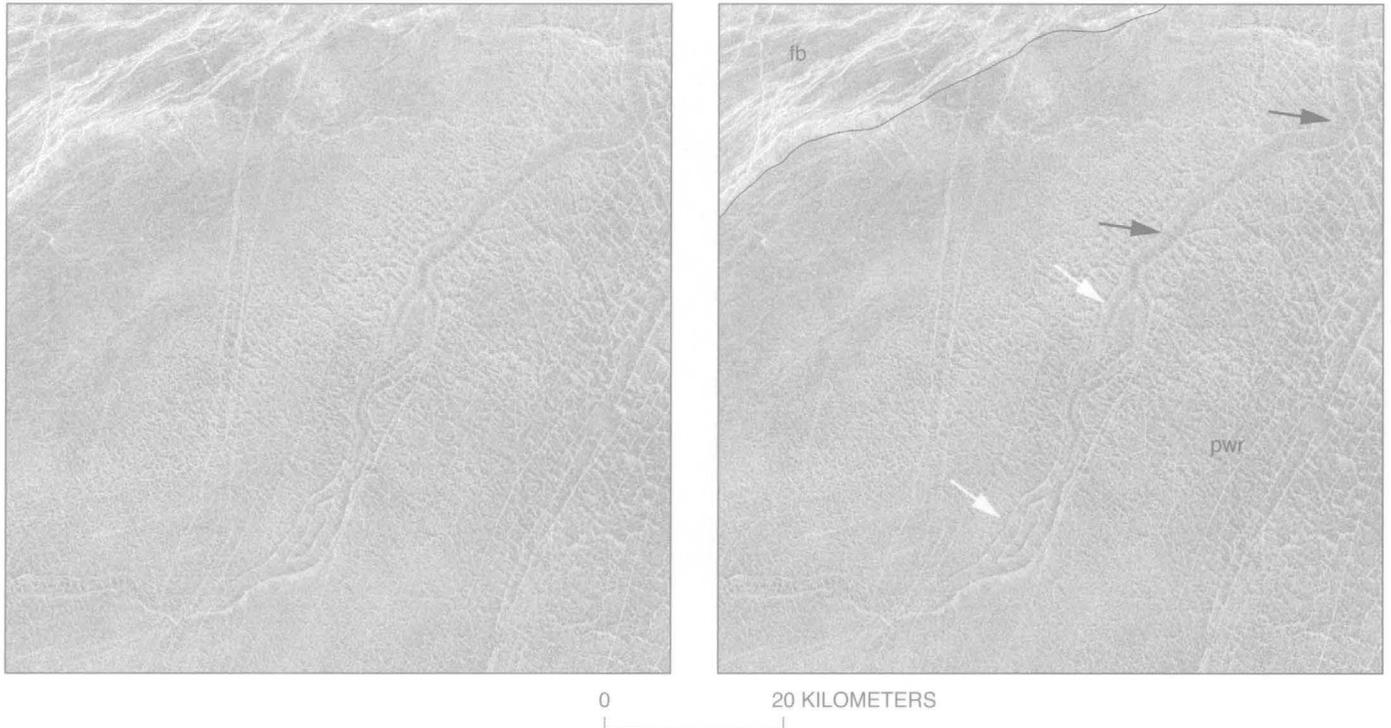
Figure 13. The northeastern part of the 200-km-long Omutnitsa Vallis canali at the northeastern flank of Beta Regio rise. It is cut into pwr plains material. The plains and canali are both deformed by wrinkle ridges. White arrows show places of canali divergence, black arrows show where canali are deformed by wrinkle ridges. Image centered at 33.3° N., 292.5° E. Size of image is about 70 by 70 km.
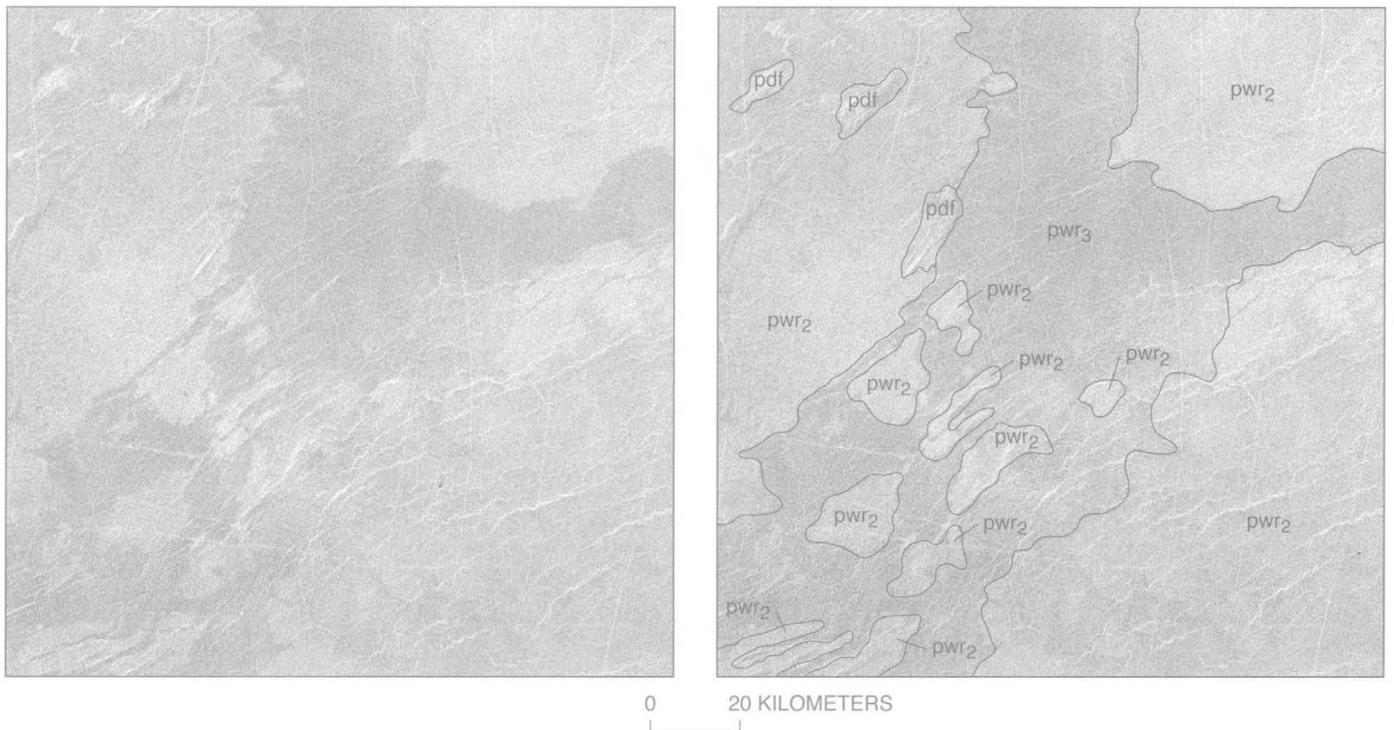

Figure 14. Member 3 of plains with wrinkle ridges (pwr3) among fields of pwr2 material. Image centered at 41.6° N., 294° E. Size of image is about 145 by 145 km.
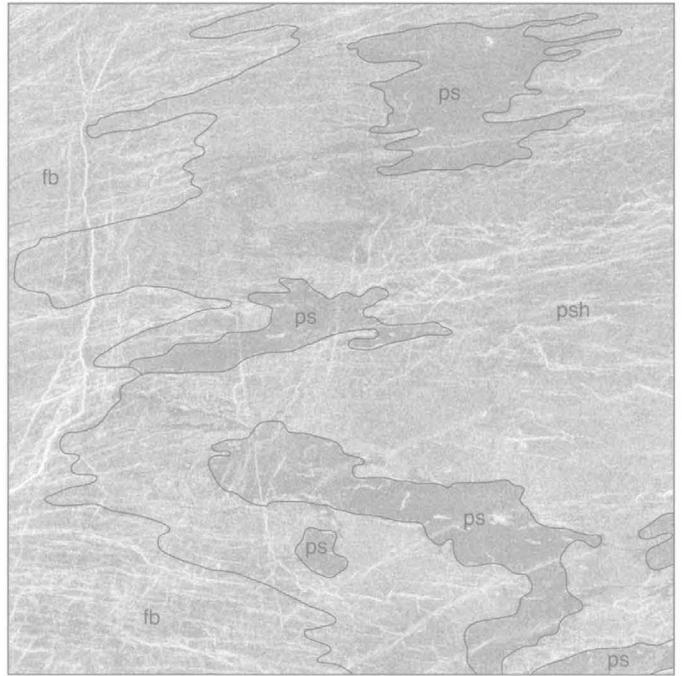
Figure 15. Small fields of smooth plains (ps) among the shield plains (psh). Image centered at 40.3° N., 285° E. Size of image is about 145 by 145 km.
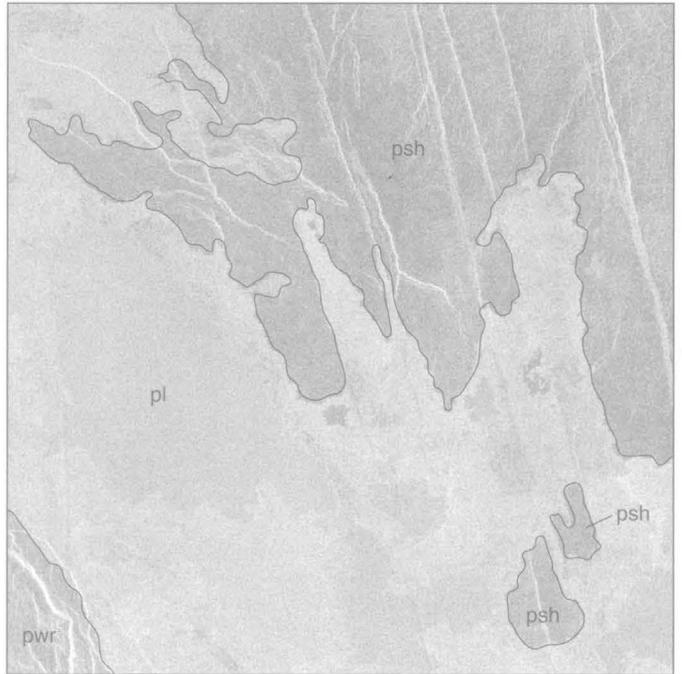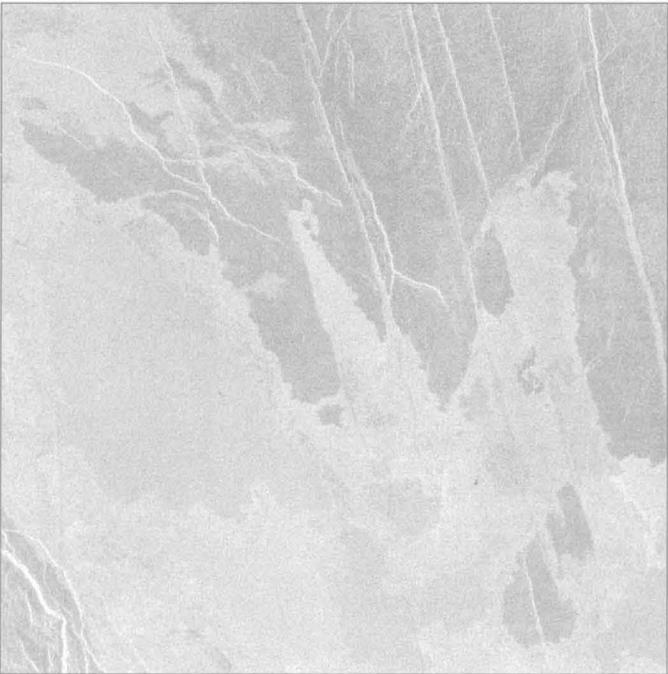

Figure 16. Lobate plains material (pl) on the northwestern slope of Theia Mons. Pl lavas overlie and embay units psh and pwr. Image centered at 28.3° N., 280.2° E. Size of image is about 145 by 145 km.

27
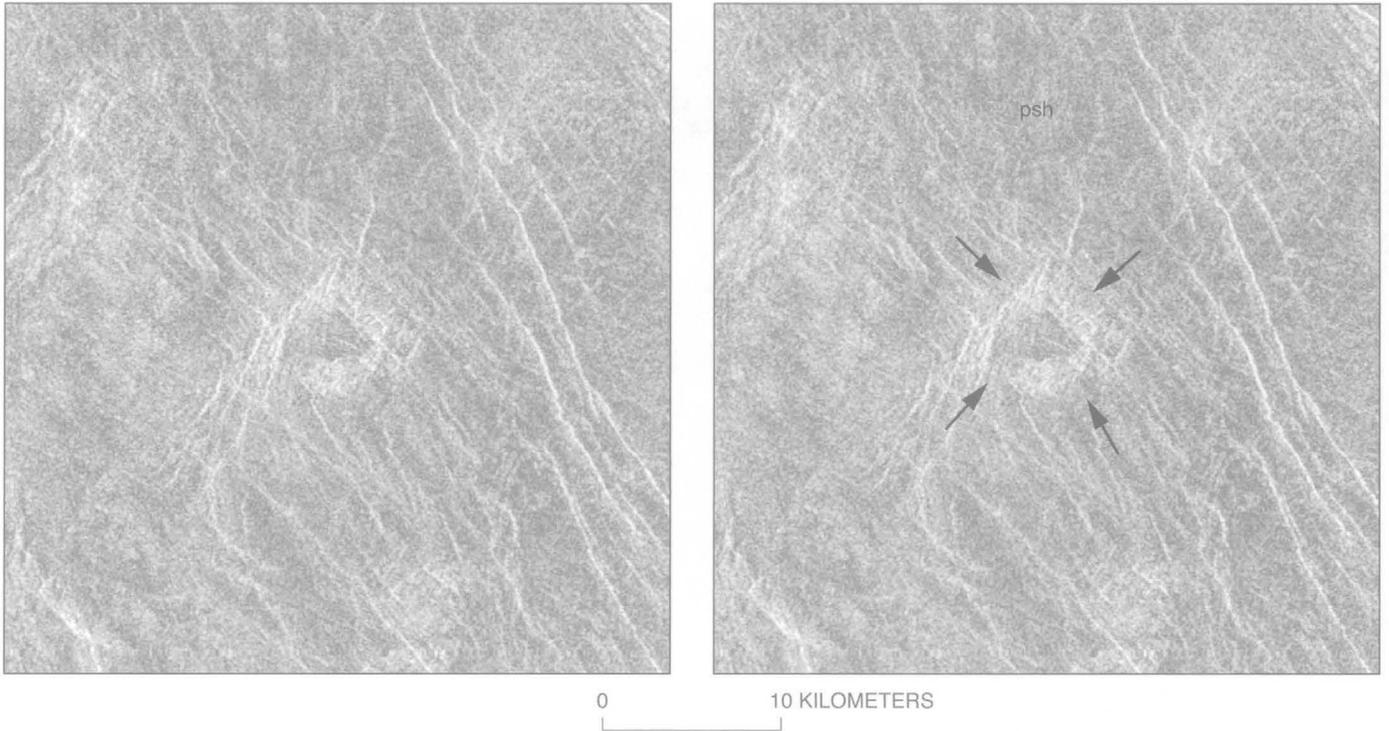
Figure 17. The crater Aigul, whose rim (marked by arrows) is deformed by northeast-trending fractures similar to those in unit pdf and the northwest-trending fractures similar to those in unit fb. Crater appears embayed and partly flooded by the psh material that relates it to unit c_1 (see table 1 for explanation). Image centered at 38.2° N., 280.4° E. Size of image is about 35 by 35 km.
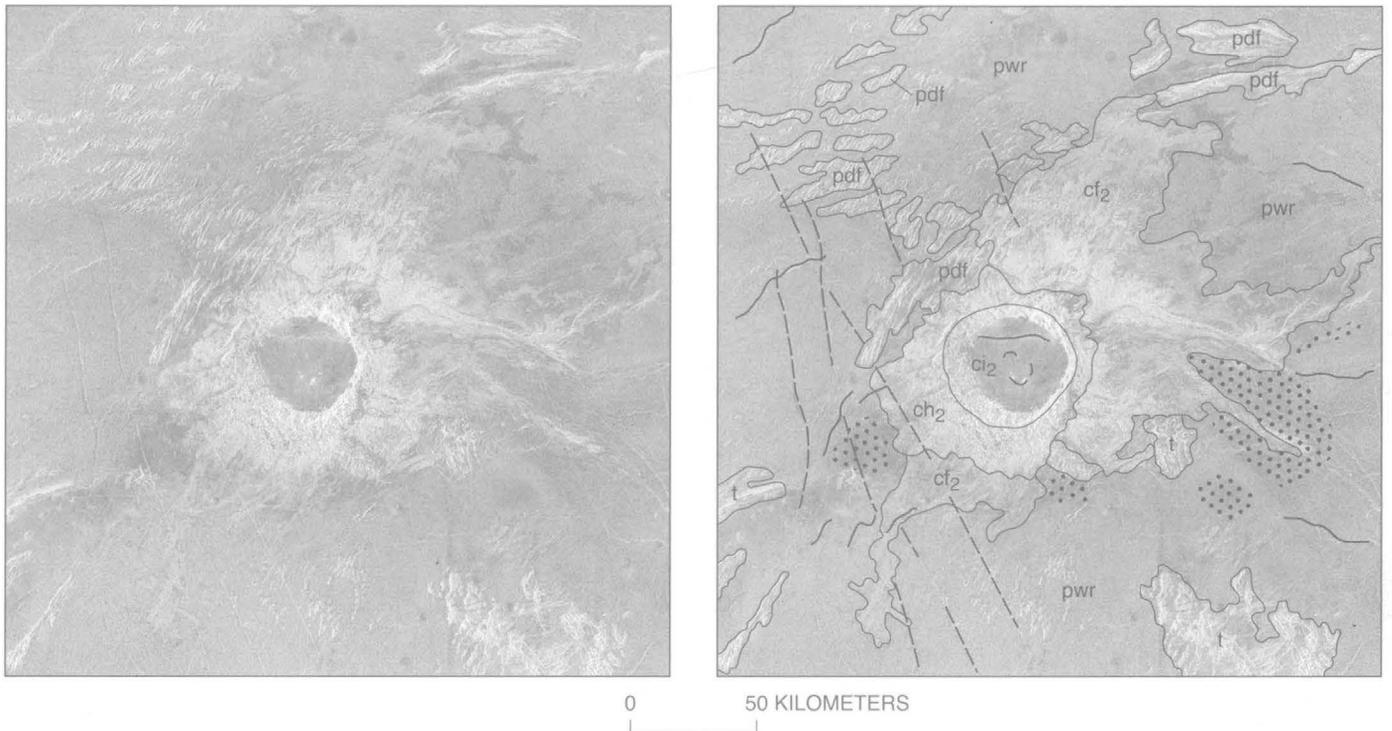
Figure 18. The crater Deken with its faint radar-dark halo (denoted by dotted areas) that relates it to unit c_2 (see table 1). The northern part of the crater floor is deformed by wrinkle ridges, whose morphology and orientation are similar to those wrinkle ridges of the surrounding pwr plains. Dashed lines show the location of grabens. Southwest of the crater its ejecta outflow buries one of the graben and is cut by another graben. Image centered at 47.1° N., 288.4° E. Size of image is about 260 by 260 km.
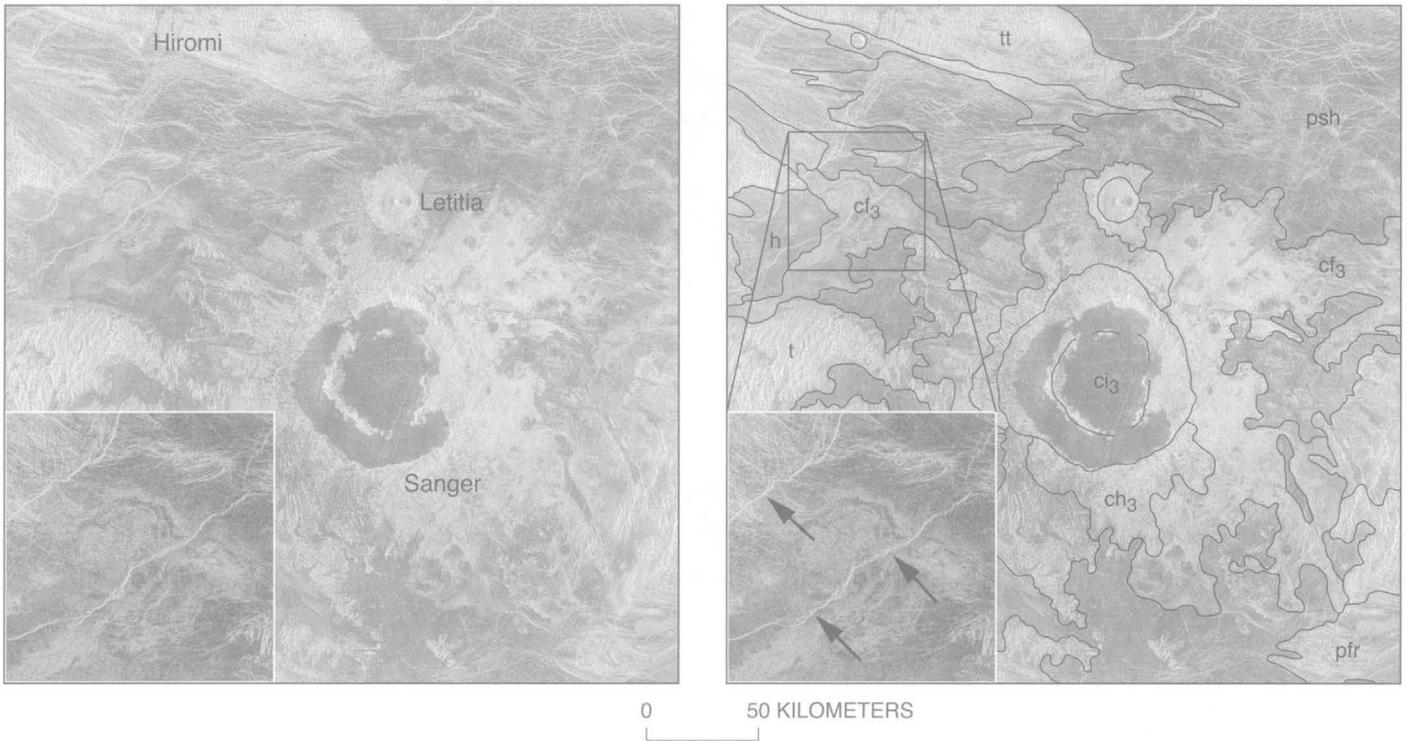
Figure 19. The crater Sanger whose ejecta outflows are cut by faults (shown in white boxes) branching from the Devana Chasma rift zone. The faults are marked by black arrows in the inset figure. This crater has a prominent radar dark halo that classifies its materials as unit c_3 (see table 1 for explanation of c_1, c_2, and c_3). Materials of the crater Sanger are divided into three facies: intracrater materials (ci_3), hummocky ejecta (ch_3), and ejecta outflows (cf_3). Although the potential halo of the crater Letitia is not seen on the background of ejecta and halo of Sanger, Letitia is classified as c_3 because it is superposed on Sanger's ejecta. The crater Hiromi is classified as c_2 because it has no noticeable radar-dark halo. Image centered at 33.8° N., 288.5° E. Size of image is about 300 by 300 km.
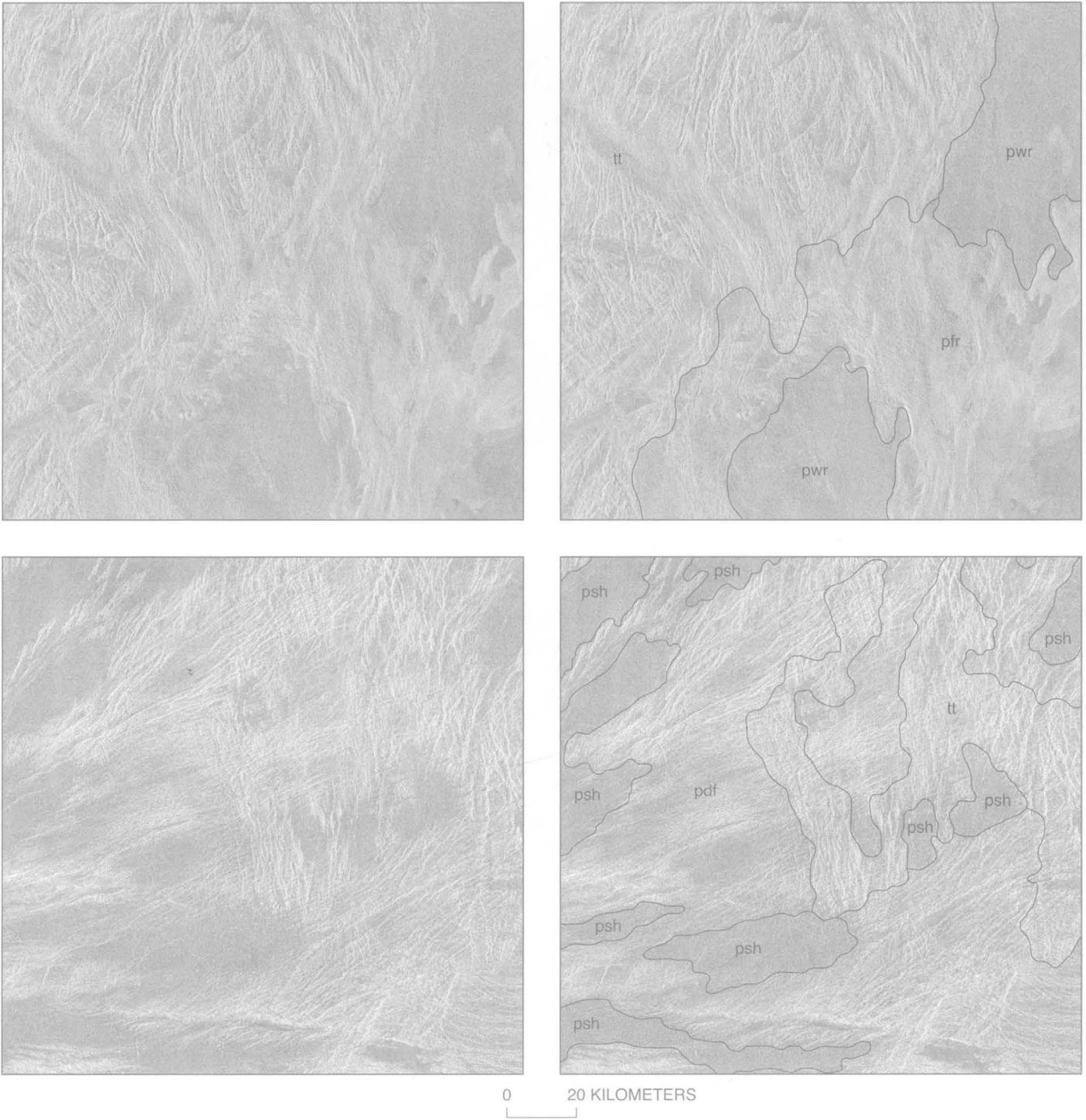
Figure 20. Tessera transitional terrain (tt) formed as a result of fracturing of the material units pfr (top) and pdf (bottom). All three units, tt, pfr and pdf, are embayed by pwr and psh plains. Images centered at 27° N., 297.2° E. and 46.5° N., 294.5° E., correspondingly. Size of images is about 145 by 145 km.

Figure 21. Fracture belt (fb) of Shishimora Dorsa in contact with pwr plains. The pwr plains embay most of the fb fractures but some fractures cut pwr material. Image centered at 38° N., 298.2° E. Size of image is about 145 by 145 km.
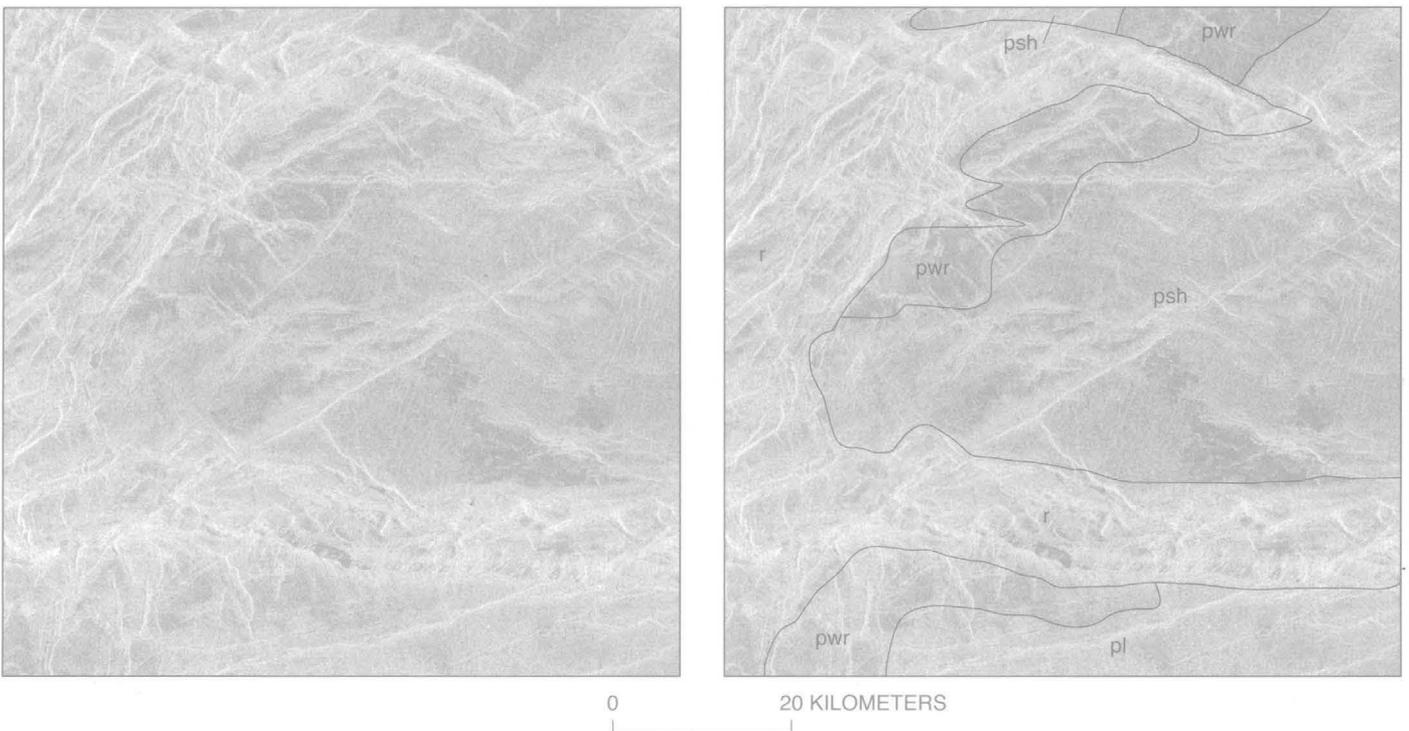
Figure 22. Part of the rifted terrain unit (r) on the northeastern slope of Theia Mons. Fractures and grabens of the r unit cut all material units (psh, pwr, and pl) of the area shown here. Image centered at 25.9° N., 285.1° E. Size of image is about 75 by 75 km.
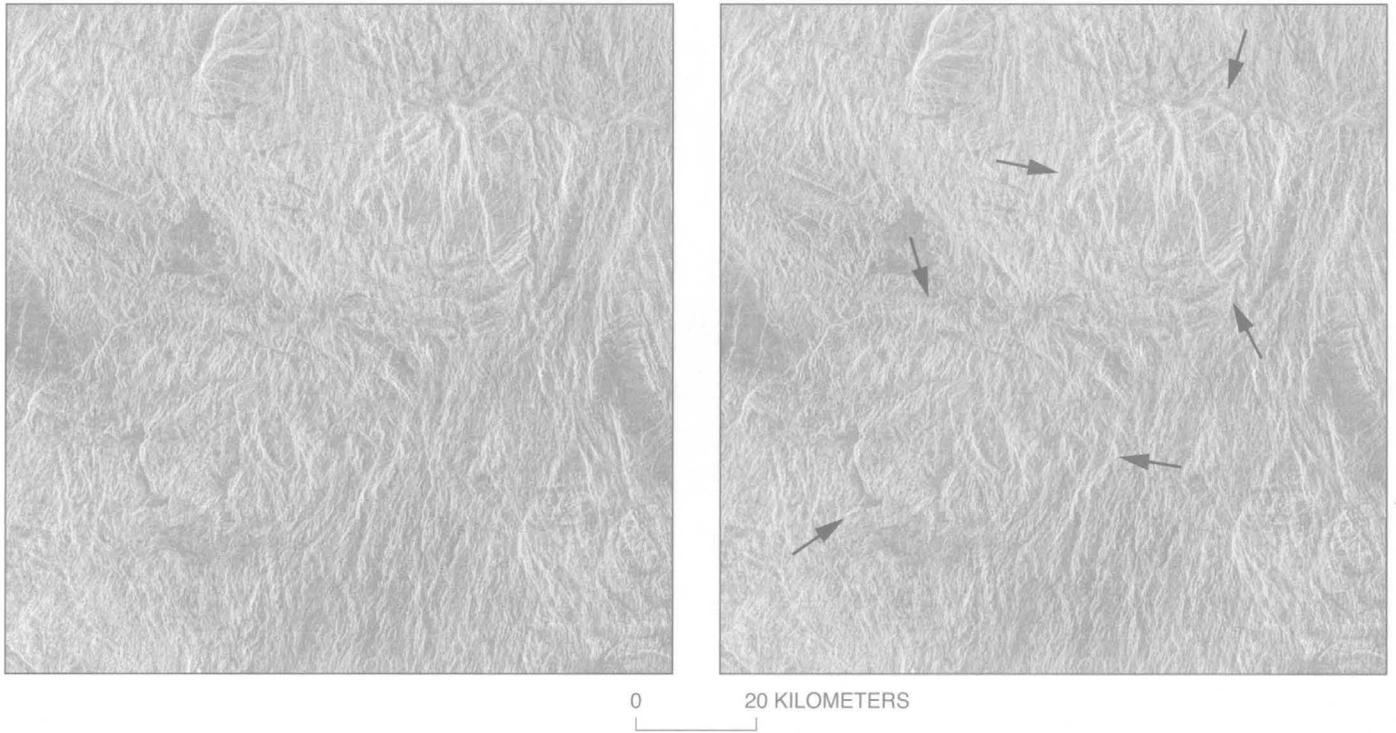
Figure 23. Tessera terrain with a local arcuate to ring-like structural pattern (arrows show two ring-like structures) on the southeastern flank of Rhea Mons. Image centered at 31.1° N., 285.3° E. Size of image is about 110 by 110 km.
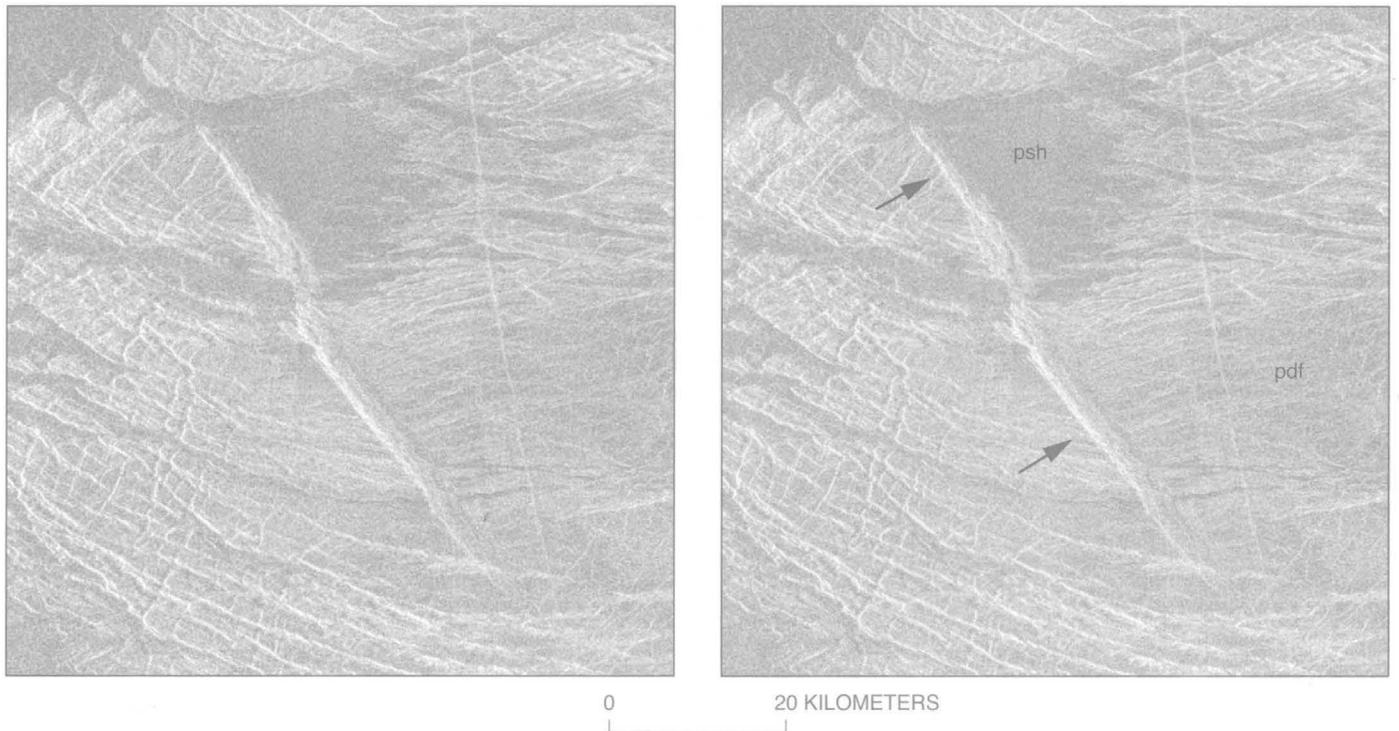
Figure 24. A broad ridge (denoted by arrows) deforming material of the densely fractured plains (pdf). The ridge is very similar to those deforming unit pfr. The pdf unit in the left part of the image is deformed by grabens. Unit pdf and most of its structures are embayed by the material of unit psh. Image centered at 46.5° N., 296.7° E. Size of image is about 80 by 80 km.

Table 1. *List of impact craters of the V–17 Beta Regio quadrangle, Venus. Coordinates and diameters (D) are from Schaber and others (1998)*

[WR, wrinkle ridges; F, young post-regional-plains fractures; halo types are: CH, clear radar-dark halo; FH, faint halo; NH, no halo; Obs, potential halo obscured by ejecta of other crater. fract., pdf-type fractures. Geologic ages of craters described in "Geologic History" section of pamphlet.]

No.	Name	Latitude (deg)	Longitude (deg)	Diameter (km)	Superposed on	Superposed by	Halo type	Geol. age
1	Esmeralda	48.44	296.6	22.9	pdf, psh, pwr	nothing	CH	c_3
2	Deken	47.13	288.48	48	t, pdf, pwr, F	WR	FH	c_2
3	Samantha	45.56	281.68	16.9	pwr, WR	nothing	FH	c_2
4	Zvereva	45.36	283.12	22.9	pwr	F	CH	c_3
5	Unnamed	43.8	290.5	1.4	pwr, WR, F	nothing	FH	c_3
6	Daphne	41.3	280.4	15.5	fb, psh	nothing	CH	c_3
7	Cholpon	40.03	290	6.3	pdf, pwr, F	nothing	CH	c_3
8	Unnamed	39.8	289.8	1.3	pdf	nothing	NH	c_3
9	Anya	39.5	297.8	18.1	pwr	nothing	CH	c_3
10	Lenore	38.69	292.2	15.5	pwr	nothing	CH	c_3
11	Sasha	38.34	277.79	4.6	psh	nothing	FH	c_2
12	Aigul	38.2	280.4	6	pdf?	pdf fract., psh	NH	c_1
13	Lida	36.6	273.9	20.3	fb, psh	nothing	CH	c_3
14	Hiromi	35.21	287.3	6	pfr, psh	F	NH	c_2
15	Letitia	34.54	288.66	17.5	psh, Sanger CH	nothing	Obs	c_3
16	Sanger	33.77	288.56	83.6	t, psh, pwr	r	CH	c_3
17	Wazata	33.6	298.3	13.9	tt, pwr	nothing	FH	c_2
18	Balch	29.9	282.91	40	psh	r	NH	c_2
19	Truth	38.68	287.75	47.3	t, pdf, pwr, WR, ps	nothing	FH	c_2
20	Nalkowska	28.14	289.95	22.2	psh, pwr, ps	nothing	FH	c_2
21	Raisa	27.5	280.3	13.5	pwr?	pl	FH	c_2
22	Unnamed	27.3	277	3	psh	nothing	CH	c_3
23	Degu	27.3	289.8	5.5	psh, pwr	nothing	FH	c_2
24	Olga	26.1	283.8	15.5	pwr, r	r	CH?	c_2
25	Tako	25.11	285.27	10.7	psh, pl	nothing?	FH	c_2

Table 2. *Percentage of unit areas in the V–17 quadrangle.*

Unit	Percent of area
t	5.11
pdf	4.67
pfr	5.15
psh	26.15
pwr_1	10.58
pwr_2	10.61
pwr_3	0.19
pwr_u	9.36
all pwr units	30.74
pl	5.46
ps	0.15
cu	0.99
tt	10.34
fb	8.78
r	2.46
Total of units	100